Untangling tau hyperphosphorylation in drug design for neurodegenerative diseases

Michael P. Mazanetz and Peter M. Fischer

Abstract | Aggregation of hyperphosphorylated tau is one of the characteristic neuropathological lesions of Alzheimer's disease and other neurodegenerative disorders. Pharmacological modulation of tau hyperphosphorylation might represent a valid and feasible therapeutic strategy for such disorders. Here, we consider recent evidence supporting the validity of the three most relevant kinases affecting tau hyperphosphorylation — GSK3β, CDK5 and ERK2 — as drug targets and describe progress in the design of inhibitors for these kinases.

Microtubule
Cytoskeletal structure that is required for normal neuronal processes such as axonal transport and neurite outgrowth. Microtubules are polymers of α- and β-tubulin dimers.

Alzheimer's disease
A degenerative disease of the brain resulting in prominent cognitive and behavioural impairment. It is the most common cause of dementia in older people and affects more than 30 million people worldwide.

Amyotrophic lateral sclerosis
A neurological disorder (also known as Lou Gehrig's disease) that is caused by the degeneration of nerve cells that control voluntary muscle movement, leading to muscle weakness and atrophy.

Centre for Biomolecular Sciences and School of Pharmacy, University of Nottingham, University Park, Nottingham NG7 2RD, UK. Correspondence to P.M.F. e-mail: peter.fischer@nottingham.ac.uk
doi:10.1038/nrd2111

Tau is a microtubule-associated protein expressed throughout the central nervous system (CNS), but predominantly in neuronal axons. Partially phosphorylated tau in the normal adult brain contains sequence motifs that promote association with tubulin, which leads to stabilization of microtubules. However, pathological hyperphosphorylation of these motifs prevents tubulin binding and thereby results in the destabilization of microtubules[1] (FIG. 1).

The longest adult tau isoforms contain as many as 79 serine and threonine residues where phosphorylation can potentially occur, although only about 30 of these seem to function as actual phosphorylation sites under normal physiological conditions[2]. Tau hyperphosphorylation, aggregation and formation of the filamentous form of the tau protein (paired helical filaments or PHF-tau) are all observed in Alzheimer's disease (AD), and a total of 25 sites where abnormal phosphorylation takes place have been identified[3]. The misfolding of hyperphosphorylated tau leads to the formation of insoluble neurofibrillary tangles (NFTs)[4]. It has long been believed that NFTs were responsible for the cytotoxic effects of tau, but recent findings suggest that this might not be the case: using transgenic mice expressing a repressible human tau variant it was observed that although neuron numbers stabilized and memory function recovered upon tau suppression, NFTs continued to accumulate[5]. This raises the possibility that PHF-tau, and perhaps other soluble lower-mass hyperphosphorylated tau aggregates, might induce neurodegeneration owing to loss of the normal function of these tau forms rather than accumulation of toxic NFTs[6,7].

Disorders related to tau — collectively referred to as neurodegenerative tauopathies[8] — are part of a group of protein misfolding disorders known as foldopathies[2]. Neurodegenerative diseases that are associated with tauopathy include AD, amyotrophic lateral sclerosis, Pick's disease and progressive supranuclear palsy[9–11]. The neuropathological hallmarks of AD were first reported in 1907 by Alois Alzheimer[12]. Apart from severe brain atrophy and neuronal loss in the brains of affected individuals, he found dense extracellular deposits and intracellular neuronal aggregates, which were subsequently identified as amyloid (neuritic) plaques and NFTs, respectively[4]. Amyloid plaques are extracellular accumulations of β-amyloid (Aβ) peptides that are derived from the proteolytic processing of the β-amyloid precursor protein (APP), whereas NFTs are intraneuronal accumulations of insoluble and hyperphosphorylated tau. Tau is intimately associated with β-amyloid-induced neurotoxicity[13], as hippocampal neurons cultured from tau knockout mice do not degenerate when challenged with fibrillar β-amyloid[14,15].

Although these invariant pathological hallmarks — plaques, tangles and neuronal death — all contribute to the aetiology of AD, the mechanistic relationships between these lesions remain to be unravelled. In this article, we first discuss the evidence indicating that inhibition of tau hyperphosphorylation is a viable therapeutic strategy for AD and other tauopathies, and then summarize progress in the development of inhibitors of the three most relevant kinases — GSK3β (glycogen synthase kinase 3β, also known as tau protein kinase I), CDK5 (cyclin-dependent kinase 5, also known as tau protein kinase II) and ERK2 (extracellular signal-regulated kinase 2) — that could be used to achieve this goal. Although many lead series with activity against these

© 2007 Nature Publishing Group

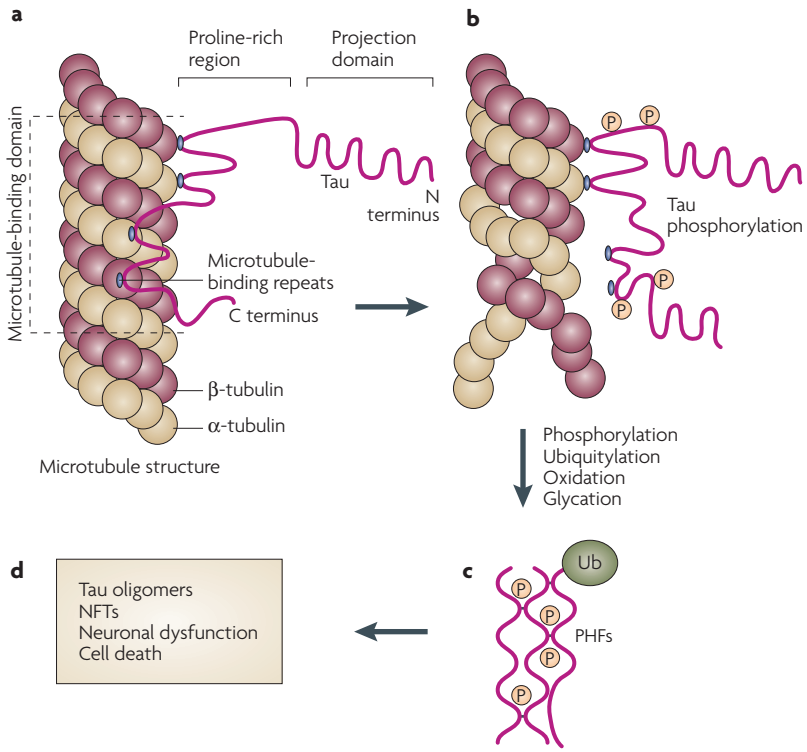

Figure 1 | **Intracellular neuronal aggregates in tauopathies. a** | Microtubules are strong cylindrical polymers composed of α- and β-tubulin that provide structural support to neurons. Tau is the major microtubule-associated protein in neurons and it stabilizes microtubule architecture through tubulin-binding motifs consisting of 18 amino-acid residues arrayed in 3 or 4 imperfect tandem repeats separated by flexible linkers of 13 variable residues. **b** | Phosphorylation at a number of serine/threonine sites flanking the microtubule-binding repeats by certain affinity-regulating kinases, including GSK3β, CDK5 and ERK2, as well as phosphorylation by other kinases in the repeat region, attenuates tau binding, which results in destabilization of microtubules. **c** | Abnormally phosphorylated tau protein becomes dissociated from neuronal microtubules and accumulates in paired helical filaments (PHFs). **d** | Proteolytic processing leads to the formation of tau oligomers and insoluble aggregates called neurofibrillary tangles (NFTs). Tau in these filaments is heavily phosphorylated at several sites and crosslinked by disulphide bonds. The decrease in the association of tau with microtubules and other physiologically relevant proteins, together with the formation of PHFs, are thought to contribute to neuronal dysfunction and eventually cell death. Kinase inhibitors have been shown to prevent tau phosphorylation, so their pharmacological application might result in a reduction of NFTs.

Pick's disease
A progressive dementia that is characterized by gradual changes in character and social behaviour, or impairment of language, and is caused by the degeneration of the frontal and temporal lobes of the brain.

Progressive supranuclear palsy
A brain disease (also known as Steele–Richardson–Olszewski syndrome) that is due to the gradual loss of cells in the midbrain, leading to reduced control of walking, balance, swallowing, speaking and eye movement.

kinases are known, the structural determinants for selectivity remain poorly understood. Specificity in terms of kinase targets and CNS bioavailability will be important design principles for safe and effective new systemic agents for treating tauopathies. We also highlight results from recent medicinal chemistry and structural biology studies that offer important clues about how mono-, oligo- and pan-specific inhibitors for these kinases might be designed.

Tau hyperphosphorylation as a drug target

Tau is an *in vitro* substrate for many protein kinases, but the number of those that phosphorylate tau *in vivo* is probably much smaller and few are actually implicated in abnormal tau hyperphosphorylation[16]. The physiologically relevant serine/threonine protein kinases fall into two classes: the proline-directed and the non-proline-directed kinases. Of the sites that are phosphorylated in tau, 13 are followed by proline residues and hence are candidate phosphorylation sites for proline-directed kinases, among which GSK3β, CDK5 and ERK1/2 have received the most attention[17,18]. Relevant non-proline-directed kinases include microtubule affinity-regulating kinase (MARK) and cAMP-dependent protein kinase (PKA). Tyrosine phosphorylation of tau by Src kinases such as FYN has also been suggested to be relevant to neurodegeneration[19,20].

Recent data have implicated both GSK3β and CDK5 in aberrant tau phosphorylation and association with microtubules[21,22]. ERK2 has also been found to be deregulated in *post mortem* AD brains, and there is evidence that ERK2 is required for neurofibrillary degeneration[23]. Other stress kinases, including stress-activated C-Jun N-terminal kinase (SAPK/JNK) and p38 mitogen-activated protein kinase (p38 MAPK), have also recently been linked with tau hyperphosphorylation[18]. Furthermore, a range of kinases, including several from the MAPK family, casein kinase and calcium/calmodulin-dependent kinase II (CaMKII), may also be relevant to tau-related neurodegeneration[17]. We confine our discussion to CDK5, GSK3β and ERK2, the three kinases that are most strongly linked with tau hyperphosphorylation .

CDK5. All known CDKs require association with a regulatory subunit — usually a cyclin — for activation[24]. In the case of CDK5, these activators have been identified as the p35 and p39 proteins, which are expressed almost exclusively in postmitotic neurons[25]. CDK5/p35 knockout mouse studies have shown that CDK5 is essential not only for survival in general, but specifically for neuronal development[26,27]. Elevated cellular levels of calcium trigger the cleavage of p35 and p39 to the more stable p25 and p29 fragments by the calcium-dependent protease calpain[28,29]. These truncated forms, which seem to be downstream effectors of Aβ peptides, upregulate CDK5 activity and can therefore be regarded as neurotoxic activators of CDK5 (REFS 30–32). Indeed, deregulation of CDK5 is intimately linked with the pathological characteristics of AD[33–35].

Calpain activation, p25 accumulation, CDK5 co-localization with NFTs and elevation of CDK5 activity have all been observed directly in the AD brain[36–39]. Furthermore, the association of CDK5–p25 with pre-tangle neurons in AD brains suggests that CDK5 might be involved in the early stages of NFT formation during AD development[40]. Recent *in vivo* studies in rodent models demonstrate that progressive neurodegeneration and NFT formation are triggered by the inducible expression of p25, reinforcing the evidence that the CDK5–p25 pathway is a crucial component of AD pathophysiology[41–43]. It was demonstrated recently that transgenic mice co-expressing both mutant (P301L) human tau and p25 show an accumulation of aggregated and hyperphosphorylated tau, which is associated with GSK3, as well as increased NFTs[44]. Interestingly, overexpression of p35 in mice that also overexpress tau and CDK5 does not increase tau phosphorylation[45], whereas overexpression of p25 does[33]. Presumably this is due to the fact that p35, the CDK5

© 2007 Nature Publishing Group

Table 1a | **Physicochemical properties and predicted BBB permeability of CDK5–GSK3β–ERK2 inhibitors**

Name	Structure	CLogP*	PSA (Å²)	M_r	nON (HBA)‡	nOHNH (HBD)§	CLogP – nON‖	Predicted logBB¶
(*R*)-Roscovitine[102,125]	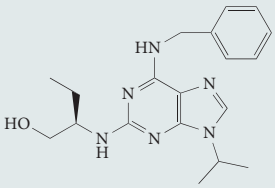	3.7	105	354	7	3	–3.3	–0.85
Aloisine A[102,110]	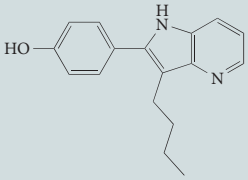	3.8	95	266	4	2	–0.2	–0.69
Indirubin-3′-oxime[102,114]	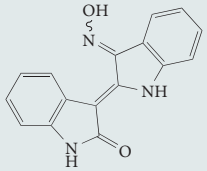	2.4	156	277	5	3	–2.6	–1.81
SB220025 (REF. 131)	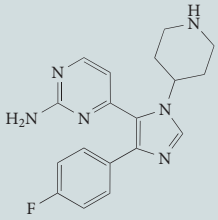	1.2	142	338	6	3	–4.8	–1.78
Pyrazolo-pyridine[111]	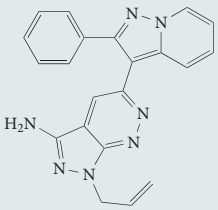	2.9	128	367	7	2	–4.1	–1.31
AR-A014418 (REF. 59)	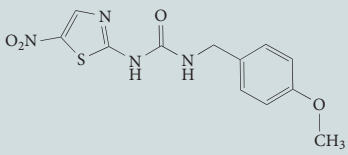	–1.1	222	308	8	2	–9.1	–3.31
Aminothiazole[158]	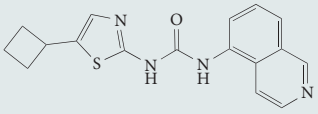	4.0	128	324	5	2	–1.0	–1.15
Alster-paullone[150,159]	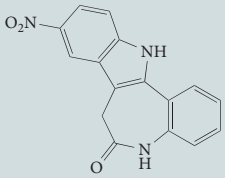	–0.5	178	293	6	2	–6.5	–2.57

*ClogP was calculated using the program Bio-Loom for Windows, Version 1.5; BioByte. The polar surface area (PSA) was determined using the SYBYL 7.2 program suite from Tripos. Values should be 1 < CLogP < 3 and PSA < 90² (better < 70²) for likely blood–brain barrier (BBB) permeability[163]. ‡The number of nitrogen and oxygen atoms (nON) in a molecule corresponds to the number of hydrogen-bond acceptors (HBA). §Similarly, the number of OH and NH functions (nOHNH) gives the number of hydrogen-bond donors (HBD). Favourable BBB permeation is predicted if M_r < 450 (better < 400), HBA < 6, and HBD < 2 (REF. 149). ‖If CLogP – nON > 0 then logBB is likely to be > –1 (REF. 163). ¶Using the formula logBB = –0.0148 PSA + 0.152 CLogP + 0.139 (REF. 164). A cut-off for BBB permeability is logBB > –1 (better > –0.3).

© 2007 Nature Publishing Group

Table 1b | **Physicochemical properties and predicted BBB permeability of CDK5–GSK3β–ERK2 inhibitors**

Name	Structure	CLogP*	PSA (Å^2)	M_r	nON (HBA)‡	nOHNH (HBD)§	CLogP – nON‖	Predicted logBB¶
Acridinyl-thiazolinone[160]	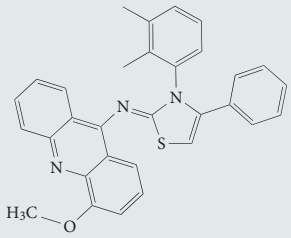	10.3	47	488	4	0	6.3	1.01
1-Aza-9-oxafluorene[161]	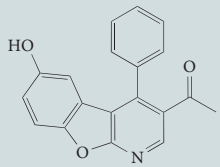	3.9	127	303	4	1	–0.1	–1.15
Bisaryl-maleimide[162]	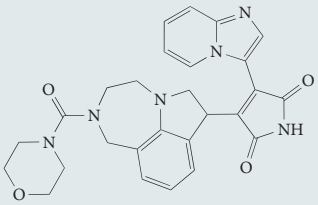	1.7	164	499	9	1	–7.3	–2.03
Indolocarbazole K252a (REF. 7) (X = O, R^1 = Me, R^2 = OH, R^3 = OMe)	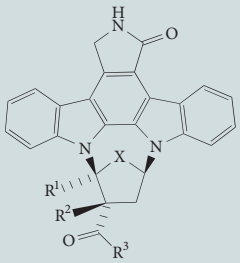	3.3	121	467	8	2	–4.7	–1.15
Indolocarbazole SRN-003-556 (REF. 7) (X = CH_2, R^1 = H, R^2 = $NH_3^+Cl^-$, R^3 = NHMe)	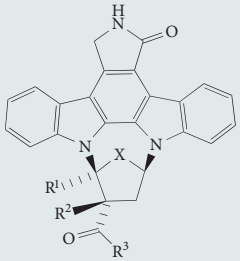	4.2	141	486	7	5	–2.8	–1.31

*ClogP was calculated using the program Bio-Loom for Windows, Version 1.5; BioByte. The polar surface area (PSA) was determined using the SYBYL 7.2 program suite from Tripos. Values should be 1 < CLogP < 3 and PSA < 90^2 (better < 70^2) for likely blood–brain barrier (BBB) permeability[163]. ‡The number of nitrogen and oxygen atoms (nON) in a molecule corresponds to the number of hydrogen-bond acceptors (HBA). §Similarly, the number of OH and NH functions (nOHNH) gives the number of hydrogen-bond donors (HBD). Favourable BBB permeation is predicted if M_r < 450 (better < 400), HBA < 6, and HBD < 2 (REF. 149). ‖If CLogP – nON > 0 then logBB is likely to be > –1 (REF. 163). ¶Using the formula logBB = –0.0148 PSA + 0.152 CLogP + 0.139 (REF. 164). A cut-off for BBB permeability is logBB > –1 (better > –0.3).

β-amyloid precursor protein
A ubiquitous membrane protein that is prominent in neurons. Proteolysis leads to the generation of β-amyloid, a 39–42 amino-acid peptide that forms amyloid plaques.

activator that predominates under normal conditions, does not co-localize with tau, whereas p25, the main pathological activator, does[16]. Tau hyperphosphorylation is also closely linked with neuronal cell apoptosis, as the microtubule binding capacity of tau isolated from apoptotic neuronal cells is markedly decreased[46,47]. Furthermore, the association with tau and the activity of CDK5 are significantly elevated in apoptotic neuronal cells[48]. The similarity between the tau hyperphosphorylation patterns observed *in vitro* in apoptotic neuronal cells and those in the AD brain indicate a connection between neuronal apoptosis and AD.

GSK3β. This multifunctional kinase is involved in the regulation of a wide range of cellular processes[13,49,50], including metabolism, cell proliferation, cardiac hypertrophy,

© 2007 Nature Publishing Group

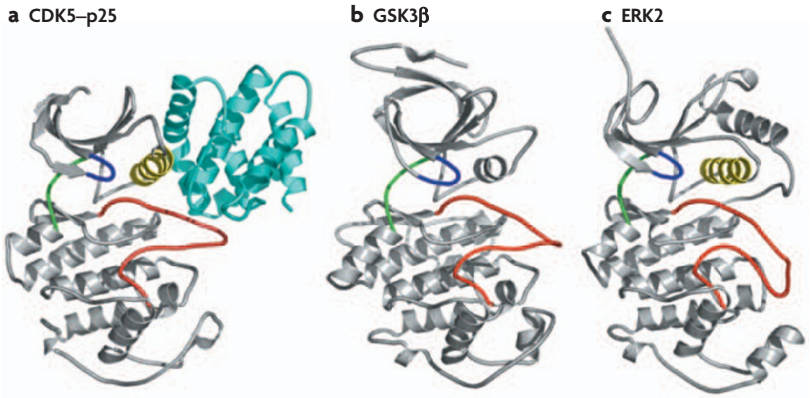

Figure 2 | **Three-dimensional protein structures of CDK5–p25, GSK3β and ERK2.** These kinases, which consist of an N-terminal domain containing mostly β-sheets and a C-terminal α-helical domain, are shown as secondary structure ribbon cartoons (grey). Common structural elements are colour-coded as follows: PSTAIRE/helix αC, yellow; activation loop (T-loop), red; hinge region, green; Gly-rich loop, blue. **a** | CDK5–p25 complex modelled from PDB (Protein Data Bank) numbers 1UNL (REF. 102) and 1H4L (REF. 103). p25 is depicted in cyan. **b** | GSK3β structure modelled from PDB numbers 1Q4L (REF. 150), 1Q5K (REF. 59) and 1I09 (REF. 152). **c** | ERK2 structure is based on PDB number 1TVO (REF. 136). Three-dimensional structure illustrations were prepared using the PyMOL program.

oncogenesis and apoptosis. Although GSK3β is perhaps best known as a potential drug target for metabolic conditions such as type-2 diabetes and insulin resistance owing to its effects on glycogen metabolism[51], it is highly expressed in the brain and is linked to a variety of CNS disease states, including ischaemic stroke, bipolar disorders, Huntington's disease and AD[52,53].

The disease association with AD was established when GSK3β was isolated from brain extracts and shown to produce PHF-like epitopes on tau. It is now clear that GSK3β contributes to β-amyloid generation and is involved in brain ageing[54]. There is strong evidence that GSK3β co-localizes preferentially with NFTs, is active in pre-tangle neurons and contributes to the formation of PHF in the AD brain[55]. GSK3β has been shown to phosphorylate tau at some of the sites that are hyperphosphorylated in PHFs, both in transfected mammalian neuronal cells and *in vivo*[56–58]. Furthermore, a potent and specific GSK3 inhibitor, AR-A014418 (TABLE 1a), was shown to inhibit tau phosphorylation at a GSK3-specific site[59]. Tau from GSK3β-transfected cells, as well as from mice expressing high levels of GSK3β, displays AD-specific epitopes[55]. CDK5 has been shown to potentiate tau phosphorylation by priming sites for subsequent phosphorylation by GSK3β[60], and CDK5 is known to regulate GSK3β-driven neuronal motility[61].

Transgenic mice with elevated GSK3β expression show increased tau phosphorylation and deficits in spatial learning[21,62,63]. Apart from its roles in tau phosphorylation, GSK3β is also involved in regulating other AD-related mechanisms[13]. GSK3β activity can be reduced through phosphorylation of Ser9 by a number of kinases, including AKT/PKB (protein kinase B). Several receptor-coupled signalling systems, such as the anti-apoptotic actions of the AKT pathway, seem to use this method of GSK3β downregulation. Furthermore, amplification mechanisms involving Ser9 phosphorylation and dephosphorylation that affect both inhibition[64] and activation[65] of GSK3β have been reported. It is therefore possible that GSK3β overexpression might actually result in downregulation of its activity, or that pharmacological GSK3β inhibition may persist after cessation of treatment. However, studies using conditional overexpression of GSK3β in forebrain neurons of transgenic mice have shown that these animals recapitulate aspects of AD neuropathology, including tau hyperphosphorylation, and that GSK3β transgene shut down restores normal GSK3β activity[66].

ERK2. ERK2 is highly expressed in neurons. This contrasts with the low number of ERK2 transcripts in sciatic nerves, which contain neuronal axons and glia but lack neuronal bodies and, therefore, neuron-specific mRNA[67]. ERK2 is also the only known kinase that stoichiometrically phosphorylates the multi-repeat domain of the middle-sized neurofilament (NF-M) *in vivo*, indicating a role for this enzyme in normal cytoskeletal regulation[68]. This finding was subsequently corroborated in functional *in situ* studies[69].

ERK2 has an important role in regulating tau functions[70] and tau phosphorylation by ERK2 decreases the affinity of tau for microtubles about 10-fold, thereby reducing the ability of tau to stabilize microtubules[1]. Phosphorylated (activated) ERK2 has been implicated in the early stages of neurofilament and tau phosphorylation in neurons and glial cells in Niemann–Pick type C (NPC), AD and in other tauopathies[71]. NPC, a disorder of cholesterol metabolism, is characterized by the accumulation of NFTs and progressive neurodegeneration. Using a transgenic mouse model of NPC, it has been demonstrated that increased tau phosphorylation at AD-relevant epitopes coincides with increases in both ERK1 and ERK2 activation[72]. In this study, no changes were observed in the levels of CDK5 and p35, or in the phosphorylation status of GSK3β. These data suggest that ERK2 activation is relevant to tau phosphorylation under neuropathological conditions.

An immunocytochemical survey of the regulatory state of ERKs in *post mortem* AD and normal brains showed that activated ERK is a prominent feature in AD, establishing a link between abnormal tau phosphorylation and oxidative stress[23]. ERK2 appears to be activated in all AD neurons that display tau and neurofilament hyperphosphorylation, suggesting an absolute requirement for ERK2 deregulation in neurofibrillary degeneration. However, unlike CDK5, ERK2 is not associated with apoptosis[71].

GSK3β, CDK5 and ERK2 are associated with APP processing. It is established that at least GSK3 is essential for Aβ-induced neurotoxicity[73]. Exposure of cultured neurons to Aβ activates GSK3, CDK5 and ERK2, leading to tau hyperphosphorylation and, ultimately, to apoptosis[74–76]. Furthermore, the production of Aβ is modulated by APP and an increase in APP phosphorylation at Thr668 by CDK5–p25 has been shown to enhance the production

© 2007 Nature Publishing Group

a

	8								18	20	31	33	47	51	55	64	80								89	127	129	131	134	144
CDK2	E	K	I	C	E	G	T	Y	G	V	K	A	K	T	E	L	V	F	E	F	L	H	Q	D	K	D	K	Q	N	L	A	D	F	G
	8								18	20	31	33	47	51	55	64	80								89	126	128	130	133	143
CDK5	E	K	I	C	E	G	T	Y	G	V	K	A	K	S	E	L	V	F	E	F	C	D	Q	D	K	D	K	Q	N	L	A	D	F	G
	27								37	39	50	52	65	69	73	82	103								112	147	149	151	154	164
ERK2	S	Y	I	C	E	G	A	Y	G	V	S	A	K	R	E	L	I	Q	D	L	M	E	T	D	K	D	K	S	N	L	C	D	F	G
	60								70	72	83	85		97	101	110	132								141	181	183	185	188	199
GSK3β	K	V	I	C	N	G	S	F	G	V	Q	A	K	–	E	M	V	L	D	Y	V	P	E	T	R	D	K	Q	N	L	C	D	F	G
										*	*	:	.	*	*	:	:	.	:	.	.	.	.	:	*	*	.	*	*	.	*	*	*	

b Active CDK2 Inactive CDK2

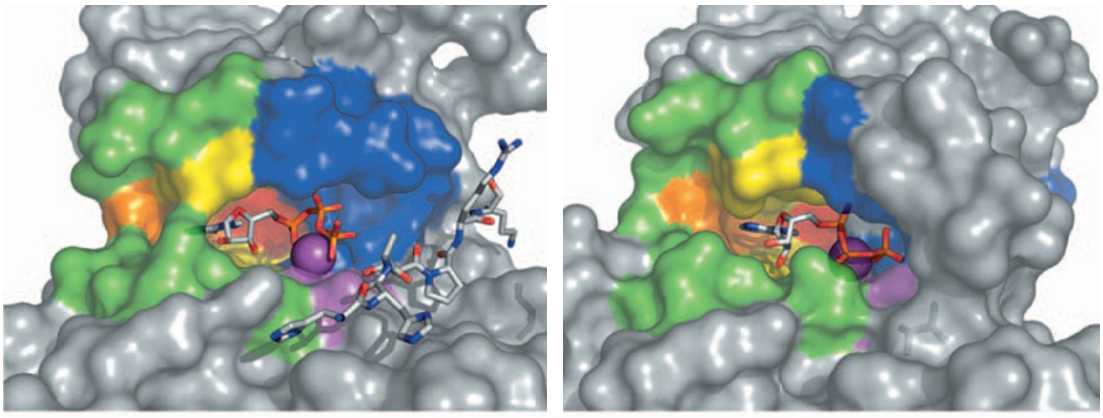

c CDK5/roscovitine GSK3β/6-Br-indirubin-3′-oxime ERK2/pyrazolo[3,4-*c*]pyridazine

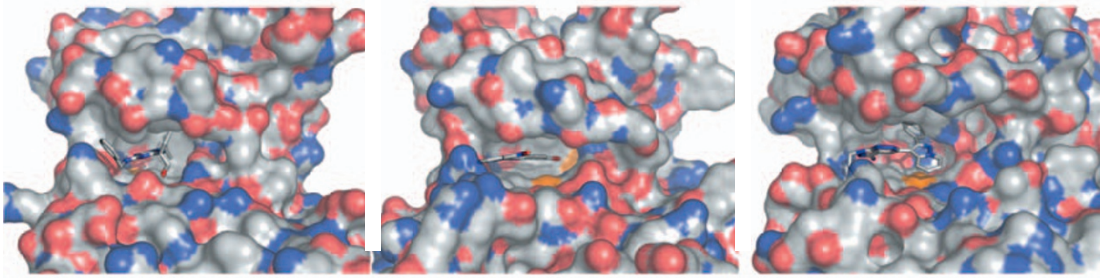

Figure 3 | **The kinase ATP-binding pocket. a** | Alignment of the residues that define the ATP-binding cleft in CDK2, CDK5, ERK2 and GSK3β shows that the four kinase sequences differ significantly at the gate-keeper residue and in the specificity surface residues, whereas the sequence is much more conserved at the subsites that interact directly with ATP. **b** | A surface representation of the ATP-binding region in CDK2 serves as a model for the recognition of ATP by CDK5, GSK3β and CDK5 . Fully activated T-loop-phosphorylated CDK2 (phosphothreonine residue indicated on the surface in yellow), which is cyclin-bound and substrate peptide-complexed, is shown on the left (PDB (Protein Data Bank) number 1QMZ (REF. 157)) and represents the catalytically competent conformation. The T loop forms a platform for the recognition of the substrate (CPK (Corey–Pauling–Koltun) sticks). In inactive kinase conformations (right) an ATP-bound structure is shown (PDB number 1HCK (REF. 134)). The opening to the ATP-binding site is wider and the phosphate site is distorted; similar conformations are observed in many inhibitor-complexed structures. Bound ATP (CPK-coloured stick model) interacts with the kinase hinge region (orange) through H-bonds that involve the adenine aminopyrimidine ring. The floor and roof of the ADP-binding site form a hydrophobic clamp (yellow) that accommodates both the adenine purine ring system and the ribose portion of ATP, while the acidic triphosphate group binds in the basic phosphate-binding site (blue). Kinases also require magnesium (purple sphere) as a cofactor for phosphotransfer from ATP to the macromolecular substrate. Two regions of the ATP-binding site that are not involved in direct contacts with ATP but that can be exploited for the design of selective inhibitors are a small hydrophobic pocket delineated by the so-called gate-keeper residue (red) at the base of the ATP-binding site and the opening to the binding cleft, sometimes referred to as the surface specificity site (green). The hinge region residues are also poorly conserved but the side chains of these residues do not protrude into the ATP-binding cleft and the interactions involve the peptide backbone. **c** | Aligned views of CDK5, ERK2 and GSK3β complexes with the most selective inhibitors are shown (CPK-coloured surfaces for kinases and stick models for inhibitors; PDB numbers 1UNL (REF. 102), 1UV5 (REF. 116) and 1WZY (REF. 111)). The shape and chemical make-up of the ATP-binding pockets in these complexes are significantly different.

© 2007 Nature Publishing Group

of Aβ[77]. Further evidence of links between extraneuronal amyloid deposition and tau pathology comes from using a transgenic mouse model of familial AD, in which elevated levels of Aβ and increased exposure of Alzheimer's-type tau phosphoepitopes correlated with deregulation of CDK5, leading to an increase in p25 levels[78]. Inhibition of CDK5 or calpain activity diminishes Aβ-induced apoptosis of primary cortical neurons[31,79], which suggests that increased calcium concentrations attributed to elevated Aβ levels stimulate the cleavage of p35 to p25 in neurons[80]. However, there is also evidence that CDK5 inhibition might augment Aβ production[81]. On the other hand, inhibition of GSK3β by lithium has been shown to protect cultured neurons against Aβ-induced neurodegeneration[82,83].

Pharmacological target validation. Recent insights into the mechanisms of neurodegeneration suggest that intervention in tau pathologies might be pharmacologically tractable, as genetic suppression of aberrant tau in transgenic models leads to recovery of neurological function[6,84]. However, until recently, no direct evidence was available to show that suppression of tau hyperphosphorylation with small-molecule agents would be therapeutically useful or even feasible. Several recent reports now provide such evidence. First, intrathecal administration of a calpain inhibitor not only prevented CDK5 activation, but decreased tau hyperphosphorylation and improved neurological function after spinal cord hemisection in rats[85]. Furthermore, inhibition of GSK3β by lithium ions (which have long been in clinical use for the treatment of bipolar disorder, and which inhibit GSK3β and certain CDK-unrelated kinases by competing for magnesium ions[86]) has recently been shown to correlate with reduced tauopathy and neurodegeneration *in vivo*[57,87,88]. Another study that suggests that pharmacological intervention might not only prevent tau aggregation but actually lead to resolution of preformed aggregates used small-molecule inhibitors that were discovered using an *in vitro* PHF formation assay[89,90]. The most direct evidence, however, comes from the report by Le Corre and colleagues[7] which shows that small-molecule tau hyperphosphorylation kinase inhibitors (indolocarbazole compounds in TABLE 1b) can reduce tau hyperphosphorylation and the formation of soluble aggregated tau, and prevent motor deficits on administration to transgenic mice expressing mutant human tau[91]. The compounds in question are derived from the promiscuous kinase inhibitor staurosporin and are therefore not very selective; the most potent compound SRN-003-556 was reported to inhibit at least ERK2, CDK1, GSK3β, PKA and protein kinase C (PKC) *in vitro* with K_i values of 0.1–0.6 μM (REF. 7).

So, the question remains: which of the tau phosphorylation kinases should be inhibited for optimal therapeutic effects? Although it seems that GSK3β might be the main protagonist in pathological tau hyperphosphorylation, this kinase is potentially a problematic therapeutic target because it is involved in the regulation of so many other physiological processes[53]. In particular, the role of GSK3β in the Wnt signalling pathway suggests that chronic GSK3β inhibition might be oncogenic[92]. Many cancers arise as a result of mutation of Wnt pathway components, such as mutations in the β-catenin gene. Normally, proteasomal degradation of β-catenin is promoted by GSK3β phosphorylation, and mutations in β-catenin can produce dominant negative forms that are stabilized and accumulate, leading to the development of cancers in mice.

Similarly, CDK5 and ERK2 belong to kinase families that have multiple roles in many tissues. The main problem with CDK5 inhibitors is the fact that they usually also inhibit some of the 10 other CDKs, which have important roles in regulating the cell cycle and mRNA transcription[93]. Therefore, the use of these types of inhibitors as CNS drugs might cause undesirable toxicity. Nevertheless, there are indications that selectivity for CDK5 over other CDKs might be achievable. For example, certain compounds described as indolinones have been shown to potently inhibit CDK5, without significantly affecting other CDKs — including CDK2, structurally the closest CDK5 relative — as well as other cell-death-promoting kinases such as JNK and p38 MAPK[94,95]. Unfortunately, the chemical structures of these indolinones have not been disclosed (presumably these are related to the indirubins discussed below) so it is impossible to draw conclusions that would be helpful in terms of selectivity design.

Partial modulation of more than one of the three prime tau hyperphosphorylation kinases with oligospecific inhibitors, instead of full inhibition of any one of them with mono-specific inhibitors, might result in a better therapeutic margin by maintaining effective suppression of tau hyperphosphorylation while minimizing the potential toxic effects that are associated with the complete suppression of individual non-redundant kinase functions. In the remainder of this article, we discuss the progress so far in the development of such inhibitors with varied selectivity profiles which will allow the rational design of pharmacological tools to probe these questions and provide drug candidates for the treatment of tau-related CNS diseases.

Structure-based kinase inhibitor design

At present, 518 protein kinases that catalyse the transfer of the terminal phosphate group from the cofactor ATP to a macromolecular kinase substrate are known to be encoded in the human genome[96]. The conservation of structural features within the ATP-binding cleft of kinases initially indicated that specificity for ATP site-directed inhibitors would be difficult to achieve. However, structural elucidation of kinase complexes with ATP and non-hydrolysable ATP analogues has revealed that there are regions at the periphery of, and even within, the binding cleft that ATP does not fully occupy. These regions are structurally diverse between different kinases and provide opportunities for the discovery and design of selective small-molecule ATP-competitive inhibitors[97,98].

Structural overview. CDK5, GSK3β and ERK2 are phylogenetically and structurally closely related kinases that share high sequence homology and display similar structural elements that are involved in the regulation of their activity[96,99]. These three kinases show the typical two-lobed globular kinase fold with a β-strand domain

© 2007 Nature Publishing Group

at the N terminus and an α-helical domain at the C terminus[100] (FIG. 2). ERK2 and GSK3β are both activated by phosphorylation of specific residues that are located in a well-defined region referred to as the activation loop or T loop. Phosphorylation of Thr183 and Tyr185 in the T loop of ERK2 results in a 1,000-fold enhancement of the catalytic activity of this kinase. A corresponding phosphothreonine residue is absent in GSK3β, but Tyr216 in the T loop seems to be an intramolecular autophosphorylation site that is important for GSK3β stability[53]. The main consequence of T-loop phosphorylation is a structural reconfiguration that allows optimal substrate binding. CDK5 differs from most other kinases, including other CDKs, in this respect: the apoenzyme is in a constitutively active form, and catalytic activity is enhanced following binding of regulatory partners such as p25 and p35 (REF. 101).

In all three kinases, the ATP-binding pocket is buried deep within the two lobes, the interface of which constitutes the active site cleft. When ATP binds in this cleft the γ-phosphate group projects towards the opening of the pocket, close to the kinase substrate binding

Box 1 | **Indirubins**

The general structure of the indirubin pharmacophore is depicted (panel **a**), as well as a table showing half-maximal kinase inhibition concentrations (IC_{50}) of some of the more potent indirubin derivatives that have been reported (panel **b**). Panel **c** shows a structural overlay of the ATP-binding pocket of GSK3β (yellow) and ERK2 (pink) to CDK5 (grey) containing bound indirubin-3′-oxime (green; first entry in table). The residues associated with CDK5 are labelled.

In the hinge region, two hydrogen bonds (H-bonds) between indirubin ligands and the carbonyl oxygen of $E81_{CDK5}$ ($D104_{ERK2}$, $D133_{GSK3β}$) and $C83_{CDK5}$ (M_{ERK2}, $V_{GSK3β}$) can invariably be observed. As expected, substitution at N1 abolishes inhibitory activity towards both CDK5 and GSK3β as this precludes the formation of these essential H-bonding interactions. The hinge region also provides an H-bond donor to the C2 carbonyl oxygen of indirubins from the backbone NH of residues $C83_{CDK5}$, $M106_{ERK2}$ or $V135_{GSK3β}$. The oxime function further improves binding within the ATP pocket through H-bonding with a neighbouring water molecule and the backbone carbonyl oxygens of $D86_{CDK5}$ ($T138_{GSK3β}$, $D109_{ERK2}$) and $Q130_{CDK5}$ ($S151_{ERK2}$, $Q185_{GSK3β}$). Selectivity towards CDK5 and GSK3β over ERK2 is due to unfavourable interactions of the oxindole benzene ring with the polar gate-keeper residue $Q103_{ERK2}$ and steric clashes with $Leu154_{ERK2}$, which projects upwards into the adenine-binding domain. Both CDK5 and GSK3β possess hydrophobic gate-keeper residues ($F80_{CDK5}$, $L132_{GSK3β}$) that can form corresponding favourable interactions. Modest selectivity towards GSK3β over CDK5 is due to the fact that the smaller $L132_{GSK3β}$ gate keeper is better able than $F80_{CDK5}$ to accommodate the oxindole benzene ring, especially if it is further substituted as in 6-bromoindirubin-3′-oxime, in which the 6-bromo substituent forms optimal hydrophobic interactions with $M101_{GSK3β}$ and $L132_{GSK3β}$. In addition, an adjacent pocket in GSK3β (formed by M101, L130 and F201) and ERK2 (A50, K52 and I101) can further accommodate bulky ligands, a feature that is absent from CDK5.

Replacement of the 3′-oxime with a carbonyl function results in substantial loss of activity against both CDK5 and GSK3β because of loss of favourable interactions. However, selectivity for CDK5 over GSK3β can be achieved in this context by the introduction of a polar sulphonic acid substituent at C5 ($R^2 = SO_3H$); further improvement of this selectivity is obtained by placement of a hydrophobic bromo substituent at C5′ (R^4 = Br). In the kinase-bound conformations, the sulphonic acid substituent lies very close to where the α-phosphate of ATP normally interacts with $D144_{CDK5}$ ($D200_{GSK3β}$, $D165_{ERK2}$) and $K33_{CDK5}$ ($K85_{GSK3β}$, $K52_{ERK2}$). The improved CDK5 selectivity is likely to result from a steric clash of the sulphonic acid group with the large $C199_{GSK3β}$ residue, which angles the inhibitor ligand towards the hydrophobic $V90_{GSK3β}$ above the plane of the molecule. In CDK5, the smaller $A143_{CDK5}$ can better accommodate the bulky sulphonic acid group. Additional hydrophobic bromo substituents at positions C5 and C5′ (R^2 and R^4) are detrimental for activity across the series. The bulky 5-bromo substituent interacts unfavourably with the polar $D86_{CDK5}$ and $D109_{ERK2}$ residues, whereas in GSK3β this residue is the smaller and less polar T138.

a

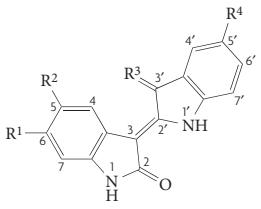

b

Substituents				IC_{50} (μM)		
R^1	R^2	R^3	R^4	*CDK5*	*GSK3β*	*ERK2*
H	H	NOH	H	0.1	0.022	>100
Br	H	NOH	H	0.083	0.005	>10
H	SO_3H	NOH	H	0.005	0.08	ND
H	H	O	H	5.5	0.6	ND
H	SO_3H	O	H	0.065	0.28	ND
H	SO_3H	O	Br	0.08	4	ND
H	Br	O	Br	200	0.25	ND
H	Br	O	H	0.25	0.055	ND

c

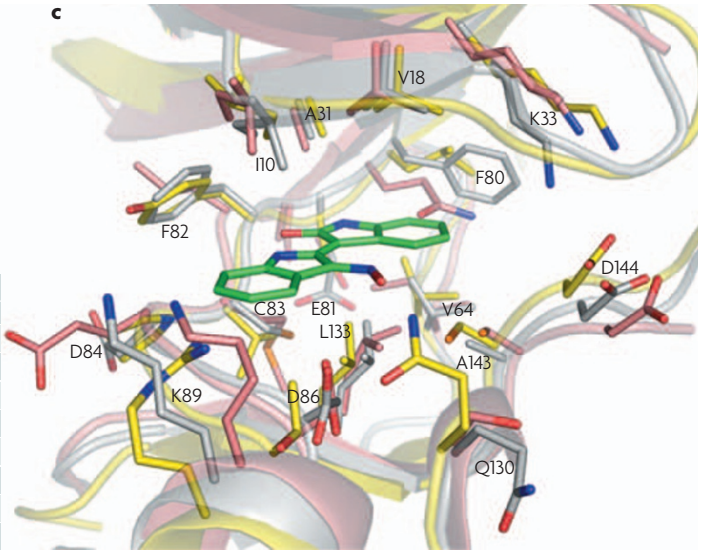

Structures are modelled from Protein Data Bank numbers 1UNH (REF. 102), 1Q41 (REF. 150), and 1TVO (REF. 140). ND, not determined.

© 2007 Nature Publishing Group

region. There are a number of highly conserved amino-acid residues clustered in the active site that are essential for ATP-binding and catalysis (FIG. 3).

Insights into inhibitor design from crystal structures. The deregulation of kinases in many pathological conditions has stimulated an active search for selective inhibitors. The development of such compounds has been aided by detailed knowledge of the ligand interactions with the ATP-binding pocket of the kinases in question gained from X-ray crystallography studies[97,98]. However, crystal structures provide a static picture of bound ligand–kinase complexes and thus give few clues as to how protein flexibility can be exploited for the purposes of specificity. Comparison of the various published complex structures of CDK5, GSK3β and ERK2 with the inhibitors discussed below shows that such flexibility exists and that even the ATP-binding site is adaptive. Furthermore, some structures may be misleading because the crystallized protein does not fully represent the physiological kinase. A relevant example is CDK5 — when a residue within its ATP-binding cleft was mutated (Asp144Asn) to improve protein expression levels, the resulting recombinant enzyme was inactive[102,103].

The design of inhibitors that specifically target inactive kinase conformations, such as the receptor tyrosine kinase (BCR–ABL) inhibitor imatinib, has recently shown much promise[104]. These so-called type-2 inhibitors — in contrast to type-1 inhibitors that can bind to both active and inactive kinase states — also bind in the ATP site but extend into an allosteric site that arises in some kinases as a result of the DFG (Asp-Phe-Gly) motif of the T-loop folding away from the catalytically competent state. Such inhibitors prevent kinase activation and usually possess potent cellular activity because they recognize and promote kinase conformations that have low affinity for ATP[105]. Such 'DFG-out' conformations are not usually crystallographically observed in the absence of type-2 inhibitors. For this reason, type-2 leads are difficult to design rationally and none is currently known for the kinases under discussion here. CDK-related kinases are believed to be unable to assume DFG-out inactive conformations, although type-2 inhibitors of CDK-related aurora kinases have recently been reported[106].

Kinase inhibitors of CDK5, GSK3β and ERK2

A large number of inhibitors that bind to the ATP pocket of various kinases have been described, including many that are more or less selective for CDKs and GSK3. Three prominent CDK5- and GSK3β-inhibitory pharmacophores are the 3′-substituted indolinones[107], especially those known as indirubins[108], the 2,6,9-trisubstituted purines[109] and the aloisines[110]. In the following sections we describe some of the salient features that determine their potency and selectivity using the known structure–activity relationships (SARs) of these three compound classes.

All of these compounds were originally discovered as CDK inhibitors and they differ in their overall selectivity profile. Apart from CDKs, indirubins generally also inhibit GSK3β, whereas most of the purines also inhibit ERK2. It has been noted that ERK2 is significantly different to most other kinases, apart from its close structural and functional homologue ERK1, and possesses an unusually restrictive ATP-binding site[7]. As a result, few ERK2 inhibitors are known and none is truly potent or selective. The aloisines are not as well characterized as a compound class as the indirubins and the purines, but they seem to hold promise as a template for the design of oligo-specific inhibitors. Aloisines contain the pyrrolo[2,3-*b*]pyrazine structure (in the discussion of these compounds we include the structurally related pyrazolo[1,5-*a*]pyridines) and are the only compound class that contains nanomolar ERK2 inhibitors[111].

Indirubins. Indirubins form part of the class of naturally occurring indigo dyes and their pharmacological properties have long been known in traditional Chinese medicine[112,113]. Planar oxime indirubin derivatives (R^3 = NOH in BOX 1) have been identified as potent and selective inhibitors of CDKs and GSK3β that seem to be practically inactive towards ERK2 (REFS 108,114–116). For example, indirubin-3′-oxime ($R^1 = R^2$ = H, R^3 = NOH) inhibits GSK3β-mediated tau phosphorylation *in vitro* ($IC_{50} \approx 100$ nM) and also effectively suppresses cellular tau phosphorylation at AD-specific sites[114].

The main interactions that account for the selectivity and potency of indirubins derive from hydrogen bonding to the kinase hinge region, contacts with the gate-keeper residue and apolar van-der-Waals bonds within the ATP-binding cleft[102] (described in BOX 1). Overall the hydrophobic van-der-Waals energies of interaction seem to account for much of the binding affinity of indirubins for CDK5 and GSK3β[115]. It is likely that the smaller binding clefts of CDK5 and GSK3β compared with the larger and more flexible ERK2 cleft result in more compact packing around the ligands, as can be observed from complex X-ray crystal structures and modelled interactions. Similar features are probably responsible for the observed selectivity of indirubins for GSK3β over CDK5. As is the case with most CDK5 and GSK3 inhibitors reported in the literature, selectivity beyond these kinases is poorly documented and thus uncertain. Because of the close structural similarity of CDK5 with both CDK1 and CDK2, CDK5 inhibitors usually inhibit CDK2 as well. This seems to be the case with many indirubins[117–120]. Furthermore, there are also reports of indirubin derivatives that possess activity against other CDKs, unrelated kinases and even non-kinase targets[120–123]. Another unfavourable property that indirubins share with many kinase inhibitors is their poor aqueous solubility, although more soluble derivatives have recently been reported[124].

Purines. Substituted purine inhibitors are based on the heterocyclic structural core present in ATP itself. However, despite being similar to ATP in this respect, purine inhibitors do not generally bind in the same manner as ATP and even comparatively insignificant chemical modifications of inhibitors can result in dramatic changes in potency[125–129] (BOX 2). The first synthetic purines to be studied as kinase inhibitors were N^6-isopentenyladenine and the 2,6,9-trisubstituted purine olomoucine[130,131]. Subsequently, many adenine- and

Pharmacophore
The steric and electronic features of a ligand that are necessary to ensure optimal interactions with a biological target structure and to trigger (or to block) its biological response.

Gate-keeper residue
A residue at the base of the ATP-binding pocket of kinases that is not itself involved in the recognition of ATP. The fact that this residue differs from kinase to kinase can be exploited in the design of selective kinase inhibitors.

© 2007 Nature Publishing Group

Box 2 | **Purines**

The general structure of the 2,6,9-trisubstituted purine pharmacophore is shown in panel **a**, as well as a table showing half-maximal kinase inhibition concentrations (IC_{50}) of some of the more potent derivatives that have been reported (ERK activities refer to ERK1 (1) or ERK2 (2)) (panel **b**). Panel **c** shows a structural overlay of the complexes between roscovitine and CDK5 (grey CPK; PDB (Protein Data Bank) number 1UNL (REF. 102)), purvalanol B and CDK2 (only ligand shown in orange, PDB number 1CKP (REF. 132)), as well as the active CDK2–ATP complex (cyan CPK; PDB number 1QMZ (REF. 151)). Panel **d** is the same roscovitine–CDK5 complex, aligned with olomoucine–ERK2 (green CPK; PDB number 4ERK (REF. 131)) and GSK3β (magenta CPK; PDB number 1I09 (REF. 152)). Ligands and residues are labelled; hydrogen bonds (H-bonds) and salt bridges are indicated by broken lines.

The order of importance of the three purine ring substituents is $R^3 > R^2 > R^1$. Furthermore, approximate additivity of the three substituents with respect to potency is observed. The C2 substituent in most cases contains a hydroxyethylamino or aminoethylamino motif capable of hydrogen bonding, the C6-substituent is usually an aniline or benzylamine and the N9 substituent is invariably a small lipophilic group. The canonical binding pose in the ATP-binding pocket of purine-based inhibitors always involves an important H-bond between the purine N6-H and the $L83_{CDK2}$ ($C83_{CDK5}$, $M106_{ERK2}$, $V135_{GSK3\beta}$) backbone oxygen of the ATP site. Amino substitution at the C2 position of the purine ring forms another H-bond to the E81 carbonyl oxygen. Overall there are comparatively fewer H-bond interactions of purines with the kinase hinge region than are observed for the indirubin scaffold.

Substituent preferences in the N6 aromatic groups (R^2 in panel **b**) differ between the anilino and benzylamino purine inhibitor series, and *para*-amino or *para*-carboxylate groups in the former have yielded the most potent analogues. Structural models show that for example, the chloro group of purvalanol A would potentially clash with $K89_{CDK2/5}$ in the active kinase state. Similarly, the *para*-carboxylate of purvalanol B prevents an H-bond that exists in the active form of CDK2 (and presumably also in CDK5) between the side-chain amine of $K89_{CDK2/5}$ in the C-terminal kinase lobe and the backbone carbonyl oxygen of $I10_{CDK2/5}$ in the N-terminal lobe (compare with FIG. 3), hence rendering these kinases inactive. The N6-benzyl groups of olomoucine and roscovitine function in a similar fashion against CDK2 and CDK5, and a corresponding H-bond in ERK2 between $K112_{ERK2}$ and $I29_{ERK2}$ is also prevented by the benzyl substituent of olomoucine as it rotates to avoid steric crowding with $L105_{ERK2}$ and $I29_{ERK2}$. In the case of the potent CDK2 and CDK5 inhibitor purvalanol B, a salt bridge between the *para*-carboxylate and the repositioned side-chain amine of $K89_{CDK2/5}$ can be observed. Other ligand scaffolds that contain arylsulphonamide functions in a similar orientation to the carboxylate of purvalanol B also show interactions with repositioned $K89_{CDK2/5}$, as well as, in some cases, with $E8_{CDK2/5}$, and are potent CDK2 inhibitors[3,133,153–156]. In CDK2, CDK5 and ERK2, the side chain of $K89_{CDK2/5}$ ($K112_{ERK2}$) seems to be able to flex away from the active site in order to accommodate bulky inhibitor groups. In this respect CDK5 and ERK2 are different from GSK3β, in which the residue corresponding to $K89_{CDK2/5}$ is $R141_{GSK3\beta}$, which is permanently salt-bridged to $E137_{GSK3\beta}$ and thus less able to move and accommodate bulky inhibitor groups protruding into the surface selectivity site at the opening of the ATP-binding cleft.

The N9-position (R^1 in panel **b**) is restrictive and only small aliphatic groups, optionally containing hydroxyl groups, are tolerated. The 9-isopropyl group appears to be optimal for CDKs, and roscovitine and purvalanols A and B lack potency against GSK3β, partly because their N9- isopropyl group is too bulky to fit inside the active site near the gate-keeper residue between residues V110, L132 and C199. In the active state of CDK2, $Q131_{CDK2}$ is rotated out of the active site and the ribose of ATP forms H-bonds to the carboxylate of $D86_{CDK2}$ and the protonated amine of $K89_{CDK2}$. Inhibitors that possess H-bond donating groups near the ribose-binding domain can disrupt the H-bond network within the protein structure. For example, olomoucine is orientated in the X-ray structure with CDK2 in such a way that the N2 hydroxyethyl group binds into the ATP-ribose pocket. Olomoucine forms H-bonds to the carboxylic acid group of $D86_{CDK2}$ ($D86_{CDK5}$, $D109_{ERK2}$, $T138_{GSK3\beta}$) and with NH of the amide $Q131_{CDK2}$ ($Q130_{CDK5}$, $Q185_{GSK3\beta}$), but there is no H-bond to the equivalent S151 residue in ERK2. ND, not determined.

a

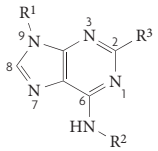

b

Inhibitor	Substituents			IC_{50} (μM)		
	R^1	R^2	R^3	*CDK5*	*GSK3β*	*ERK*
N^6-Isopentenyladenine	H	$CH_2CH{=}CHMe_2$	H	80	ND	90(1)
Olomoucine	Me	CH_2Ph	$NH(CH_2)_2OH$	3	130	30(1), 30(2)
(*R*)-Roscovitine	iPr	CH_2Ph	$NHCH(Et)CH_2OH$	0.16	220	32(1), 14(2)
Purvalanol A	iPr	3-Cl-Ph	$NHCH(iPr)CH_2OH$	0.075	>10	9(1)
Purvalanol B	iPr	3-Cl-4-COOH-Ph	$NHCH(iPr)CH_2OH$	0.006	>10	3.3(1)

c

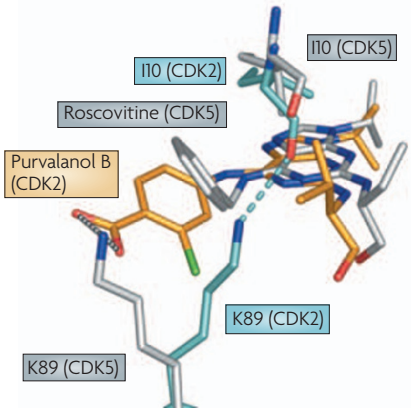

d

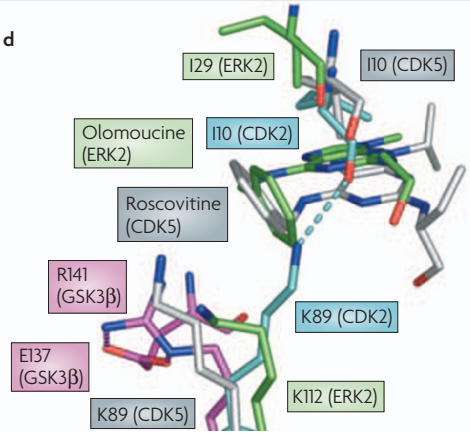

© 2007 Nature Publishing Group

guanine-based purines were developed mainly as CDK inhibitors, including roscovitine and purvalanols A and B[132–135]. Many of the interactions of these inhibitors with various kinase active sites have been determined from crystal structures of CDK2-bound ligands.

Because of the large number of known purine-based inhibitors, and owing to the fact that the rigid purine scaffold does not permit substituents to bind in overlapping regions of the active site, the kinase inhibition SARs are comparatively well understood for this pharmacophore (described in BOX 2).

Pyrrolopyrazines and pyrazolopyridines. Aloisines contain the 6-phenyl-[5*H*]-pyrrolo[2,3-*b*]pyrazine scaffold (BOX 3) and are selective inhibitors of CDK1, CDK2, CDK5 and GSK3. The most potent compound in this class is aloisine A, with reported IC_{50} values of 0.15 μM (CDK1), 0.16 μM (CDK5) and 1.5 μM (GSK3β) in functional kinase assays. Aloisine A is less potent against ERK1 (IC_{50} = 18 μM) and ERK2 (IC_{50} = 22 μM)[110]. Other aloisines are less potent towards ERKs, but the known SARs suggest that this pharmacophore might lend itself to the design of inhibitors with differential selectivity profiles (BOX 3).

Pyrazolo[3,4-*c*]pyridines, which are structurally related to the aloisines, have recently emerged as potential ERK2-selective inhibitors. The most potent compound to date (shown in BOX 3) inhibits ERK2 with an IC_{50} value of 560 nM (REF. 136).

General inhibitor design principles. An examination of the key features responsible for the potency and selectivity of known inhibitors of CDK5, GSK3β and ERK2 can be used as a guide in the design of the next generation of inhibitors. Pharmacophore maps of the ATP-binding sites can be derived from these findings (FIG. 4). These maps show that there are two main criteria that need to be met in order to yield compounds that have affinity for the ATP-binding pocket: the compounds need to bind effectively to the hinge region, through two or three H-bond donor or acceptor groups, and there must be sufficient hydrophobic interactions within the adenine-binding domain through two or more aromatic ring systems. Potent compounds feature fused heteroaromatic ring systems decorated with one or two additional cyclic systems with flexible substituents probing residues near the ribose-binding domain and within the surface specificity site. CDK5-selective compounds are generally planar and elongated structures; they often rely on breaking the H-bond between Lys89 and Ile10, either though polar contacts or steric clashes forcing Lys89 away from the opening of the ATP-binding site. Inhibitors that are designed to be selective for GSK3β need to be more compact and have less bulky groups near the gate-keeper residue than either CDK5 or ERK2 inhibitors. Furthermore, GSK3β-selective compounds often require an H-bond acceptor feature close to the ribose-binding domain that can facilitate the interaction with more distal residues though water molecules. ERK2 inhibitors require flexibility between ring systems and H-bond donor groups near the phosphate-binding domain for potency.

Other mechanisms for inhibition

The search for kinase inhibitors to date has been dominated by ATP-competitive small-molecule leads; however, alternative strategies also seem to be feasible. The first ATP-non-competitive GSK3β inhibitors that have been described are 2,3-disubstituted thiadiazolidinones and structurally related compounds[137]. Although the exact mode of kinase inhibition remains unclear, it could involve a binding site that, when occupied, interferes with T-loop conformation and substrate binding, but covalent interaction of these thiol-reactive compounds with a unique active site cysteine ($Cys199_{GSK3β}$) is the more likely explanation for the observed inhibition kinetics and kinase selectivity[138,139]. Other compounds such as thienyl and phenyl α-halomethyl ketones that have been reported to inhibit GSK3β non-competitively with respect to ATP presumably work in the same way[140].

ATP-non-competitive, but tau-competitive, inhibitors of CDK5 have also recently been reported, suggesting that inhibition of substrate binding might be a a feasible design strategy[141]. In fact, inhibitors that bind in the ATP cleft but also extend into the substrate-binding domain might offer greater kinase selectivity. Computational modelling studies aimed at the identification of the precise substrate-binding domain in CDK5 have revealed that salt-bridge formation from a Lys residue in peptide substrates to Asp86 and Asp92 of CDK5 is important for peptide binding[142]. These residues lie within the surface specificity site of CDK5, and ATP-site inhibitors that interact with these residues can be designed.

Because of the unique activation mechanism of CDK5, peptide inhibitors derived from the regulatory subunit of p35 are being pursued[143,144]. Specifically, a truncated form (residues 154 to 279) of p35 was found to bind with high affinity to CDK5, inhibiting, rather than activating, its kinase activity; this peptide is referred to as CDK5-inhibitory peptide (CIP)[145]. Transfection of cells with CIP specifically inhibits CDK5-mediated tau phosphorylation[146]. Furthermore, it was recently demonstrated that neuronal infections with CIP suppress aberrant tau phosphorylation and Aβ-induced apoptosis; surprisingly, this is due to inhibition of abnormally activated CDK5–p25 complexes, as normal CDK5–p35 complexes are not affected[147]. The reasons for this specificity are not clear, but it is possible that the N-terminal domain of p35, which is absent in p25, might obstruct CIP access to the CDK5 active site. Because of the specificity of CIP, not only for CDK5 versus other kinases, but for the neuropathologically relevant form of CDK5, targeting the CDK5–p25 protein–protein interaction might be especially attractive.

Alternative inhibitory approaches might also be possible in the case of ERK2. Specific and effective high-affinity substrate recognition by mitogen-activated protein kinases, including ERK2, involves docking sites that are removed from the phosphorylation site[148]. Although the docking sites that are relevant to tau as a substrate have not yet been characterized, this might represent an interesting line of investigation.

© 2007 Nature Publishing Group

Box 3 | **Pyrrolo[2,3-*b*]pyrazines and pyrazolo[1,5-*a*]pyridines**

The conserved substructure of these compounds is shown in red (panel **a**). Assuming that aloisine A (pyrrolopyrazine compound; magenta CPK model in panel **b**) binds to ERK2 in a similar fashion as to CDK5, an overlay with the pyrazolopyridine (green CPK) and ERK2 (grey CPK with a mobile M106 backbone residue in yellow CPK) reveals different binding poses for the two compounds: the observed hydrogen bonds (H-bonds) with the kinase hinge region ($L105_{ERK2}$, $M106_{ERK2}$) involve N4 and N5-H of the pyrrolopyrazine system for aloisine A, but one of the nitrogens and the NH_2 of the pyrazolopyridazine rather than the conserved pyrazolopyridine system in the latter case (H-bonds indicated by broken lines). The unsubstituted phenyl group of the pyrazolopyridine compound optimally occupies a small hydrophobic pocket adjacent to the gate-keeper residue present in ERK2 (panel **c**); this pocket is smaller in CDK5 (panel **e**) and practically absent from GSK3β (panel **f**), which explains why the pyrazolopyridine compound, unlike aloisine A, is ERK2-selective (inhibitors and proteins shown as grey CPK space-filling models and mesh surfaces, respectively). Structures are modelled from PDB (Protein Data Bank) numbers 1UNG (REF. 102), 3ERK (REF. 131) and 1WZY (REF. 111).

As observed with practically all CDK–GSK3–ERK inhibitors, aloisine A forms the familiar H-bond interactions with the kinase hinge region. Here, these H-bonds involve N4-H and N5 of the inhibitor and both the backbone amide NH and oxygen of $C83_{CDK5}$. In the D144N mutant CDK5 crystal structure of aloisine A, the N1 nitrogen forms H-bonds with K33, E51, N144 and two water molecules. A stronger H-bond interaction through the water molecules can be predicted for the wild-type D144 residue. The *n*-butyl chain is not well resolved in the crystal structure, which suggests that there is a high degree of freedom of movement associated with this alkyl chain[102]. The phenol hydroxyl is directed out of the binding pocket and makes suboptimal interactions with surface-specific residues. The reduced potency with respect to ERK1 and ERK2 can be rationalized in terms of the less favourable interaction between the polar gate-keeper residue ($Q103_{ERK2}$) and the pyrazine system of the ligand (panel **d**) as compared to hydrophobic interactions for CDK5 and GSK3β ($F80_{CDK5}$, $L132_{GSK3β}$). Linear planar ligands are poorly tolerated by ERK2 as the length of the binding pocket is about 2 Å shorter than that of CDK5, as measured from the gate-keeper residue ($F80_{CDK5}$, $Q103_{ERK2}$) to the surface-specific Lys residue ($K89_{CDK5}$, $K112_{ERK2}$).

Other aloisines are less potent but the known structure–activity relationships suggest that this pharmacophore might lend itself to the design of inhibitors with differential selectivity profiles. Whereas substitution at both positions b and d (panel **a**) with either chloro or methoxy resulted in loss of activity, monosubstitution at position a, b or c with OH and OMe was productive. Selectivity can apparently be controlled through the choice of substituents at position c on the aryl ring. Thus, large hydrophobic groups favour GSK3 and CDK1 versus CDK5, whereas small groups such as fluoro, methyl and cyano improve potency towards CDK5 without a significant gain in selectivity. Interestingly, removal of an H-bond donor function by methylation of N5 was not completely detrimental to potency but resulted in enhanced CDK5 selectivity.

Pyrazolo[3,4-*c*]pyridines, which are structurally related to the aloisines, have recently emerged as potential ERK2-selective inhibitors and the most potent compound found so far is shown (panel **a**). Despite the chemical similarity, the binding pose of this compound in the kinase ATP-binding site does not seem to be related to that of the aloisines. Unlike practically all other known CDK–GSK3β–ERK inhibitors, which tend to be flat molecules, the two fused heterocyclic systems present in the pyrazolo[3,4-*c*]pyridines are not coplanar. This scaffold twist allows the formation of a highly complementary interaction with the unique features of the ERK2 ATP-binding pocket. Potency and selectivity for ERK2 probably also arises through interactions of the inhibitor allyl group with the ERK2 hinge region. Unlike the equivalent residues in CDK5 and GSK3β, $M106_{ERK2}$ can rotate out of the binding pocket in order to accommodate this group[111].

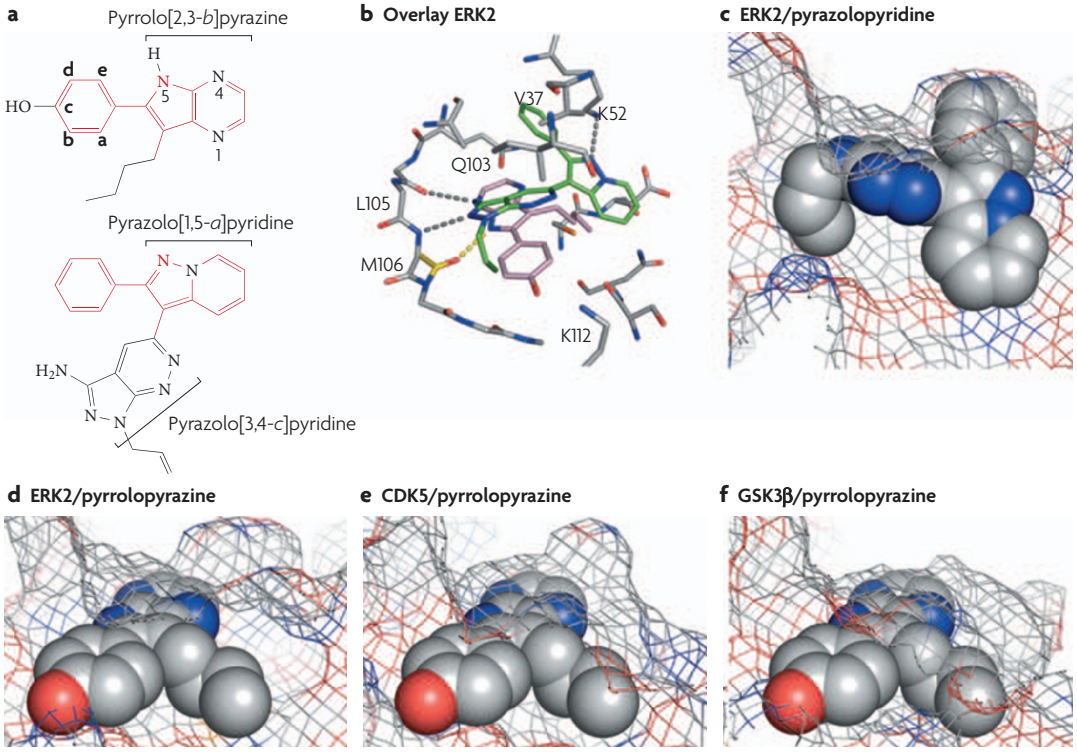

© 2007 Nature Publishing Group

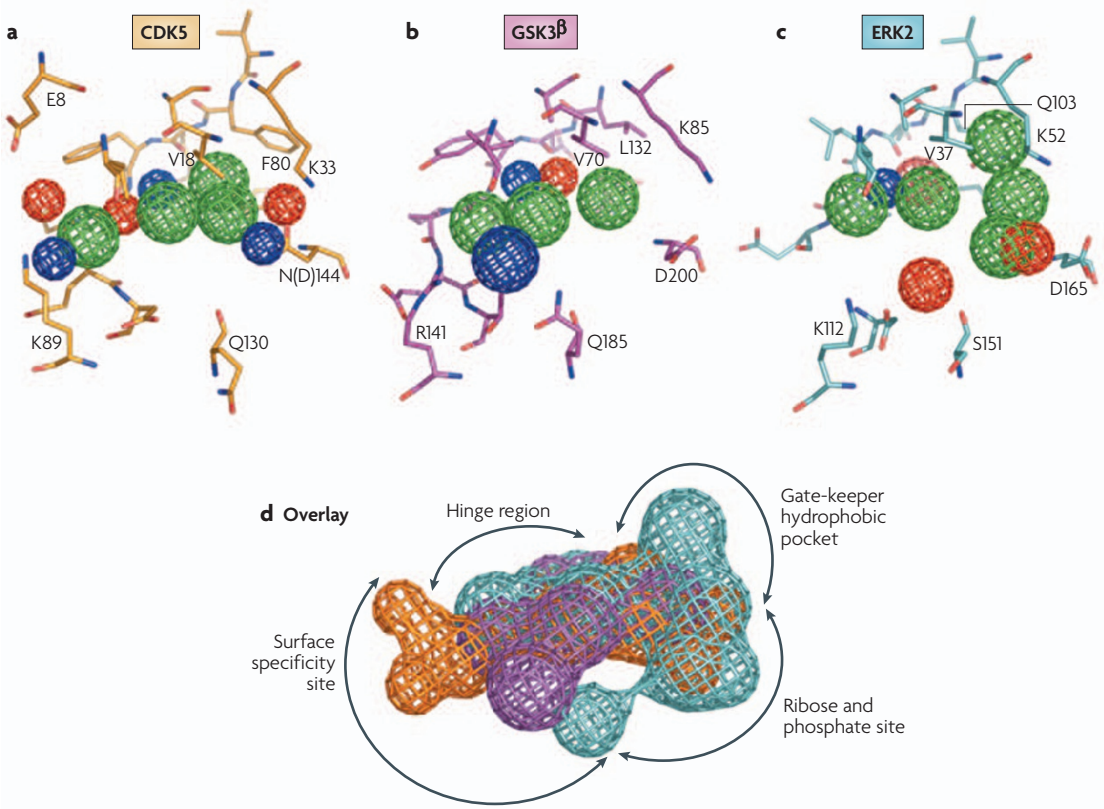

Figure 4 | **Pharmacophore maps of CDK5, GSK3β and ERK2. a–c** | The main residues lining the ATP-binding pocket of the three kinases are shown as stick models and the prominent pharmacophore features that have yielded potent inhibitors of each kinase are indicated with mesh spheres. Regions that are occupied by hydrophobic and aromatic portions of these inhibitors are depicted as green spheres and those where inhibitors commonly display H-bond donor and acceptor functions are in red and blue, respectively. **d** | An overlay of the surfaces of these pharmacophore elements for each kinase (CDK5, orange; GSK3β, magenta; ERK2, cyan) shows that potency and selectivity determinants differ significantly.

CNS bioavailability

For application in neurodegenerative diseases, kinase inhibitor drugs will have to be able to reach the CNS from systemic circulation by crossing the blood–brain barrier (BBB). The tightness of the epithelia that form the BBB effectively precludes paracellular transport, and transcellular diffusion is rendered difficult by the presence of special metabolic enzymes and efflux pumps in epithelial cells. For these reasons, the physicochemical properties required of a compound to be BBB-permeant — that is, to be capable of crossing cell membranes rapidly and escaping metabolism — are significantly more restrictive than those needed to ensure bioavailability in other tissues.

Because most kinase inhibitors are ATP-competitive, they have to contend with high (mM) cellular ATP concentrations. Kinase inhibitor lead optimization has traditionally been driven by a need for high affinity to ensure adequate dose potency. Potency is also important in terms of kinase selectivity — compounds with high nanomolar and micromolar kinase K_i values are usually promiscuous. Generally, such optimization has been successful and many inhibitors with nanomolar and even picomolar biochemical kinase inhibitory potency have been developed. However, in many cases this has given rise to highly lipophilic compounds with poor aqueous solubility. To counteract this propensity, solubilizing groups are frequently appended as part of the optimization process, so drug candidate molecules with balanced potency and solubility properties tend to be comparatively large molecules. This issue can usually be addressed to ensure the intestinal permeability required for oral bioavailability. However, BBB permeability tends to correlate with reduced molecular mass (M_r is less than 450), rigidity and reduced polar surface area (few H-bond acceptor and especially H-bond donor functions result in a polar surface area of 70 to 90 Å^2).

At present, almost nothing is known (at least in the public domain) about the BBB permeability of CDK5–GSK3β–ERK2 inhibitors. Calculated physicochemical properties for some of the compounds discussed above, as well as representatives from some other relevant pharmacophores, are summarized in TABLE 1. In most cases, comparatively poor BBB permeability is predicted. In fact the only compound with a predicted positive logBB (log $[\text{compound}]_{\text{brain}}/[\text{compound}]_{\text{plasma}}$) value, the acridinyl-thiazolinone derivative, is unlikely to be drug-like owing to excessive lipophilicity. The fact that the M_r criterion for BBB permeability is not violated by most of the compounds is probably a reflection of the fact that most have

© 2007 Nature Publishing Group

not yet been potency- and selectivity-optimized, a process that is almost invariably accompanied by increases in mass. Nevertheless, some pharmacophores, such as the aloisines, might hold promise as CNS drug leads.

The study from Le Corre *et al.* referred to previously disclosed BBB-permeant inhibitors of tau hyperphosphorylation[7]. The compounds in question are the indolocarbazole analogues K252a and SRN-003-556 shown in TABLE 1. With SRN-003-556, a maximal concentration of 1.8 μM (corresponding plasma C_{max} of 3 μM; that is, logBB = –0.22) was detected in mouse brain 1 hour after oral dosing at 30 mg per kg. This exceeded bioactive *in vitro* concentrations, and sufficient exposure to allow pharmacological activity was achieved using oral dosing of 10–20 mg per kg twice a day in the transgenic tau mouse model. Apparently SRN-003-556 has better BBB permeability than K252a. This is presumably due to the primary amino function that is present in SRN-003-556 but not in K252a, as compounds that are basic under physiological conditions ($7.5 \leq pK_a \leq 10.5$) are more likely to be BBB permeant[149]. The fact that SRN-003-556 would not have been predicted to have appreciable BBB permeability (TABLE 1) illustrates the fact that this property is notoriously difficult to predict. Clearly, imparting appropriate physicochemical properties to lead compounds, while maintaining biochemical potency and selectivity, will pose a significant additional hurdle in the discovery of drug candidates.

Conclusions and perspectives

The search for inhibitors of protein kinases has recently culminated in the registration of several such agents for cancer therapies. The challenge now is to develop kinase inhibitors for other therapeutic indications where an urgent need for effective new treatments exists. Neurodegenerative diseases, which are highly debilitating, constitute one such indication. As discussed here, there is good evidence indicating that targeting the kinases responsible for tau protein hyperphosphorylation, one of the causal events in the development of several neurodegenerative disorders, including AD, should be able to arrest — and maybe even reverse — the degeneration that is due to tau protein aggregation. Because the main tau phosphorylation kinases CDK5, ERK2 and especially GSK3β, regulate many other physiological functions apart from tau phosphorylation, it will be important to design kinase inhibitors that minimize the potential toxicity arising from inhibition of such off-target functions, while maximizing effective suppression of tau hyperphosphorylation. On the basis of the current body of knowledge about relevant protein kinase inhibitors, molecules with varying kinase inhibition selectivity profiles and appropriate bioavailability properties might be designed as pharmacological tools and, hopefully, drug candidates for the treatment of neurodegenerative tauopathies.

1. Drechsel, D. N., Hyman, A. A., Cobb, M. H. & Kirschner, M. W. Modulation of the dynamic instability of tubulin assembly by the microtubule-associated protein tau. *Mol. Biol. Cell* **3**, 1141–1154 (1992).
2. Buee, L., Bussiere, T., Buee-Scherrer, V., Delacourte, A. & Hof, P. R. Tau protein isoforms, phosphorylation and role in neurodegenerative disorders. *Brain Res. Rev.* **33**, 95–130 (2000).
3. Anderton, B. H. *et al.* Sites of phosphorylation in tau and factors affecting their regulation. *Biochem. Soc. Symp.* **67**, 73–80 (2001).
4. Hardy, J. The relationship between amyloid and tau. *J. Mol. Neurosci.* **20**, 203–206 (2003).
5. SantaCruz, K. *et al.* Tau suppression in a neurodegenerative mouse model improves memory function. *Science* **309**, 476–481 (2005).
Shows that after the suppression of transgenic tau, memory function recovered and neuron numbers stabilized, but suggests that NFTs are not sufficient to cause cognitive decline or neuronal death in the transgenic model used.
6. Trojanowski, J. Q. & Lee, V. M. Pathological tau: a loss of normal function or a gain in toxicity? *Nature Neurosci.* **8**, 1136–1137 (2005).
7. Le Corre, S. *et al.* An inhibitor of tau hyperphosphorylation prevents severe motor impairments in tau transgenic mice. *Proc. Natl Acad. Sci. USA* **103**, 9673–9678 (2006).
First report of a BBB-penetrating kinase inhibitor preventing motor deficits in a tau transgenic mouse model by reducing soluble aggregated hyperphosphorylated tau.
8. Lee, V. M., Goedert, M. & Trojanowski, J. Q. Neurodegenerative tauopathies. *Annu. Rev. Neurosci.* **24**, 1121–1159 (2001).
9. Julien, J. P. Amyotrophic lateral sclerosis: unfolding the toxicity of the misfolded. *Cell* **104**, 581–591 (2001).
10. Kuljis, R. O. Alzheimers Disease. *emedicine* <http://www.emedicine.com/neuro/topic13.htm> (2005).
11. Semple, D., Smyth, R., Burns, J., Darjee, R. & McIntosh, A. *Oxford Handbook of Psychiatry* (Oxford Univ. Press, 2005).
12. Alzheimer, A., Stelzmann, R. A., Schnitzlein, H. N. & Murtagh, F. R. An English translation of Alzheimer's 1907 paper, "Uber eine eigenartige Erkankung der Hirnrinde". *Clin. Anat.* **8**, 429–431 (1995).
13. Grimes, C. A. & Jope, R. S. The multifaceted roles of glycogen synthase kinase 3 in cellular signaling. *Progr. Neurobiol.* **65**, 391–426 (2001).
14. Takashima, A. *et al.* Presenilin 1 associates with glycogen synthase kinase-3 and its substrate tau. *Proc. Natl Acad. Sci. USA* **95**, 9637–9641 (1998).
15. Mandelkow, E. M. *et al.* Tau domains, phosphorylation, and interactions with microtubules. *Neurobiol. Aging* **16**, 355–362 (1995).
16. Johnson, G. V. & Stoothoff, W. H. Tau phosphorylation in neuronal cell function and dysfunction. *J. Cell Sci.* **117**, 5721–5729 (2004).
17. Churcher, I. Tau therapeutic strategies for the treatment of Alzheimer's disease. *Curr. Top. Med. Chem.* **6**, 579–595 (2006).
18. Lau, L. F., Schachter, J. B., Seymour, P. A. & Sanner, M. A. Tau protein phosphorylation as a therapeutic target in Alzheimer's disease. *Curr. Top. Med. Chem.* **2**, 395–415 (2002).
19. Lee, G. *et al.* Phosphorylation of tau by fyn: implications for Alzheimer's disease. *J. Neurosci.* **24**, 2304–2312 (2004).
20. Chin, J. *et al.* Fyn kinase induces synaptic and cognitive impairments in a transgenic mouse model of Alzheimer's disease. *J. Neurosci.* **25**, 9694–9703 (2005).
21. Spittaels, K. *et al.* Glycogen synthase kinase-3 phosphorylates protein tau and rescues the axonopathy in the central nervous system of human four-repeat tau transgenic mice. *J. Biol. Chem.* **275**, 41340–41349 (2000).
22. Shelton, S. B. & Johnson, G. V. Cyclin-dependent kinase-5 in neurodegeneration. *J. Neurochem.* **88**, 1313–1326 (2004).
23. Perry, G. *et al.* Activation of neuronal extracellular receptor kinase (ERK) in Alzheimer disease links oxidative stress to abnormal phosphorylation. *Neuroreport* **10**, 2411–2415 (1999).
24. Dhavan, R. & Tsai, L. H. A decade of CDK5. *Nature Rev. Mol. Cell. Biol.* **2**, 749–759 (2001).
25. Tsai, L. H., Delalle, I., Caviness, V. S. Jr, Chae, T. & Harlow, E. p35 is a neural-specific regulatory subunit of cyclin-dependent kinase 5. *Nature* **371**, 419–423 (1994).
26. Grant, P., Sharma, P. & Pant, H. C. Cyclin-dependent protein kinase 5 (Cdk5) and the regulation of neurofilament metabolism. *Eur. J. Biochem.* **268**, 1534–1546 (2001).
27. Gilmore, E. C., Ohshima, T., Goffinet, A. M., Kulkarni, A. B. & Herrup, K. Cyclin-dependent kinase 5-deficient mice demonstrate novel developmental arrest in cerebral cortex. *J. Neurosci.* **18**, 6370–6377 (1998).
28. Patzke, H. & Tsai, L.-H. Calpain-mediated cleavage of the cyclin-dependent kinase-5 activator p39 to p29. *J. Biol. Chem.* **277**, 8054–8060 (2002).
29. Hashiguchi, M., Saito, T., Hisanaga, S. & Hashiguchi, T. Truncation of CDK5 activator p35 induces intensive phosphorylation of Ser202/Thr205 of human tau. *J. Biol. Chem.* **277**, 44525–44530 (2002).
30. Ishiguro, K. *et al.* Identification of the 23 kDa subunit of tau protein kinase II as a putative activator of cdk5 in bovine brain. *FEBS Lett.* **342**, 203–208 (1994).
31. Lee, M. S. *et al.* Neurotoxicity induces cleavage of p35 to p25 by calpain. *Nature* **405**, 360–364 (2000).
32. Lew, J. *et al.* A brain-specific activator of cyclin-dependent kinase 5. *Nature* **371**, 423–426 (1994).
33. Cruz, J. C., Tseng, H. C., Goldman, J. A., Shih, H. & Tsai, L. H. Aberrant Cdk5 activation by p25 triggers pathological events leading to neurodegeneration and neurofibrillary tangles. *Neuron* **40**, 471–483 (2003).
Provides compelling evidence that *in vivo* deregulation of CDK5 by p25 has a causative role in neurodegeneration and the development of neurofibrillary pathology.
34. Patrick, G. N. *et al.* Conversion of p35 to p25 deregulates Cdk5 activity and promotes neurodegeneration. *Nature* **402**, 615–622 (1999).
35. Pei, J. J. *et al.* Accumulation of cyclin-dependent kinase 5 (cdk5) in neurons with early stages of Alzheimer's disease neurofibrillary degeneration. *Brain Res.* **797**, 267–277 (1998).
36. Lee, K. Y. *et al.* Elevated neuronal Cdc2-like kinase activity in the Alzheimer disease brain. *Neurosci. Res.* **34**, 21–29 (1999).
37. Yamaguchi, H. *et al.* Preferential labeling of Alzheimer neurofibrillary tangles with antisera for tau protein kinase (TPK) I/glycogen synthase kinase-3 β and cyclin-dependent kinase 5, a component of TPK II. *Acta Neuropathol.* **92**, 232–241 (1996).
38. Grynspan, F., Griffin, W. R., Cataldo, A., Katayama, S. & Nixon, R. A. Active site-directed antibodies identify calpain II as an early-appearing and pervasive component of neurofibrillary pathology in Alzheimer's disease. *Brain Res.* **763**, 145–158 (1997).

© 2007 Nature Publishing Group

39. Tseng, H. C., Zhou, Y., Shen, Y. & Tsai, L. H. A survey of Cdk5 activator p35 and p25 levels in Alzheimer's disease brains. *FEBS Lett.* **523**, 58–62 (2002).
40. Augustinack, J. C., Sanders, J. L., Tsai, L. H. & Hyman, B. T. Colocalization and fluorescence resonance energy transfer between cdk5 and AT8 suggests a close association in pre-neurofibrillary tangles and neurofibrillary tangles. *J. Neuropathol. Exp. Neurol.* **61**, 557–564 (2002).
41. Cruz, J. C. & Tsai, L. H. Cdk5 deregulation in the pathogenesis of Alzheimer's disease. *Trends. Mol. Med.* **10**, 452–458 (2004).
42. Takashima, A. *et al.* Involvement of cyclin dependent kinase 5 activator p25 on tau phosphorylation in mouse brain. *Neurosci. Lett.* **306**, 37–40 (2001).
43. Ahlijanian, M. K. *et al.* Hyperphosphorylated tau and neurofilament and cytoskeletal disruptions in mice overexpressing human p25, an activator of cdk5. *Proc. Natl Acad. Sci. USA* **97**, 2910–2915 (2000).
44. Noble, W. *et al.* Cdk5 is a key factor in tau aggregation and tangle formation *in vivo*. *Neuron* **38**, 555–565 (2003).
Thorough investigation linking tau and NFT phosphorylation to CDK5-p25 using transgenic mice models.
45. Van den Haute, C. *et al.* Coexpression of human cdk5 and its activator p35 with human protein tau in neurons in brain of triple transgenic mice. *Neurobiol. Dis.* **8**, 32–44 (2001).
46. Davis, P. K. & Johnson, G. V. Energy metabolism and protein phosphorylation during apoptosis: a phosphorylation study of tau and high-molecular-weight tau in differentiated PC12 cells. *Biochem. J.* **340** 51–58 (1999).
47. Davis, P. K. & Johnson, G. V. The microtubule binding of Tau and high molecular weight Tau in apoptotic PC12 cells is impaired because of altered phosphorylation. *J. Biol. Chem.* **274**, 35686–35692 (1999).
48. Zhang, J. & Johnson, G. V. Tau protein is hyperphosphorylated in a site-specific manner in apoptotic neuronal PC12 cells. *J. Neurochem.* **75**, 2346–2357 (2000).
49. Doble, B. W. & Woodgett, J. R. GSK-3: tricks of the trade for a multi-tasking kinase. *J. Cell Sci.* **116**, 1175–1186 (2003).
Summarizes GSK3 biology and provides drug target rationale for several therapeutic applications.
50. Hardt, S. E. & Sadoshima, J. Glycogen synthase kinase-3β: a novel regulator of cardiac hypertrophy and development. *Circ. Res.* **90**, 1055–1063 (2002).
51. Nikoulina, S. E. *et al.* Inhibition of glycogen synthase kinase 3 improves insulin action and glucose metabolism in human skeletal muscle. *Diabetes* **51**, 2190–2198 (2002).
52. Bhat, R. V., Budd Haeberlein, S. L. & Avila, J. Glycogen synthase kinase 3: a drug target for CNS therapies. *J. Neurochem.* **89**, 1313–1317 (2004).
53. Cohen, P. & Goedert, M. GSK3 inhibitors: development and therapeutic potential. *Nature Rev. Drug. Discov.* **3**, 479–487 (2004).
54. Yoshida, H. & Ihara, Y. Tau in paired helical filaments is functionally distinct from fetal tau: assembly incompetence of paired helical filament-tau. *J. Neurochem.* **61**, 1183–1186 (1993).
55. Johnson, G. V. & Bailey, C. D. Tau, where are we now? *J. Alzheimers Dis.* **4**, 375–398 (2002).
56. Hong, M., Chen, D. C., Klein, P. S. & Lee, V. M. Lithium reduces tau phosphorylation by inhibition of glycogen synthase kinase-3. *J. Biol. Chem.* **272**, 25326–25332 (1997).
57. Munoz Montano, J. R., Moreno, F. J., Avila, J. & Diaz Nido, J. Lithium inhibits Alzheimer's disease-like tau protein phosphorylation in neurons. *FEBS Lett.* **411**, 183–188 (1997).
58. Lovestone, S. *et al.* Alzheimer's disease-like phosphorylation of the microtubule-associated protein tau by glycogen synthase kinase-3 in transfected mammalian cells. *Curr. Biol.* **4**, 1077–1086 (1994).
59. Bhat, R. *et al.* Structural insights and biological effects of glycogen synthase kinase 3-specific inhibitor AR-A014418. *J. Biol. Chem.* **278**, 45937–45945 (2003).
60. Sengupta, A., Wu, Q., Grundke-Iqbal, I., Iqbal, K. & Singh, T. J. Potentiation of GSK-3-catalyzed Alzheimer-like phosphorylation of human tau by cdk5. *Mol. Cell. Biochem.* **167**, 99–105 (1997).
61. Morfini, G. *et al.* A novel CDK5-dependent pathway for regulating GSK3 activity and kinesin-driven motility in neurons. *EMBO J.* **23**, 2235–2245 (2004).
62. Hernandez, F., Borrell, J., Guaza, C., Avila, J. & Lucas, J. J. Spatial learning deficit in transgenic mice that conditionally over-express GSK-3β in the brain but do not form tau filaments. *J. Neurochem.* **83**, 1529–1533 (2002).
63. Lucas, J. J. *et al.* Decreased nuclear β-catenin, tau hyperphosphorylation and neurodegeneration in GSK-3β conditional transgenic mice. *EMBO J.* **20**, 27–39 (2001).
64. Zhang, F., Phiel, C. J., Spece, L., Gurvich, N. & Klein, P. S. Inhibitory phosphorylation of glycogen synthase kinase-3 (GSK-3) in response to lithium. Evidence for autoregulation of GSK-3. *J. Biol. Chem.* **278**, 33067–33077 (2003).
65. Szatmari, E. *et al.* A positive feedback loop between glycogen synthase kinase 3β and protein phosphatase 1 after stimulation of NR2B NMDA receptors in forebrain neurons. *J. Biol. Chem.* **280**, 37526–37535 (2005).
66. Engel, T., Hernandez, F., Avila, J. & Lucas, J. J. Full reversal of Alzheimer's disease-like phenotype in a mouse model with conditional overexpression of glycogen synthase kinase-3. *J. Neurosci.* **26**, 5083–5090 (2006).
67. Boulton, T. G. *et al.* ERKs: a family of protein-serine/threonine kinases that are activated and tyrosine phosphorylated in response to insulin and NGF. *Cell* **65**, 663–675 (1991).
68. Roder, H. M. & Ingram, V. M. Two novel kinases phosphorylate tau and the KSP site of heavy neurofilament subunits in high stoichiometric ratios. *J. Neurosci.* **11**, 3325–3343 (1991).
69. Veeranna, A. *et al.* Mitogen-activated protein kinases (Erk1, 2) phosphorylate Lys–Ser–Pro (KSP) repeats in neurofilament proteins NF-H and NF-M. *J. Neurosci.* **18**, 4008–4021 (1998).
70. Drewes, G. *et al.* Mitogen activated protein (MAP) kinase transforms tau protein into an Alzheimer-like state. *EMBO J.* **11**, 2131–2138 (1992).
Identifies a MAP kinase (ERK2) as being abnormally active in AD and shows that microtubule-associated protein tau is abnormally phosphorylated by this kinase.
71. Ferrer, I. *et al.* Phosphorylated map kinase (ERK1, ERK2) expression is associated with early tau deposition in neurones and glial cells, but not with increased nuclear DNA vulnerability and cell death, in Alzheimer disease, Pick's disease, progressive supranuclear palsy and corticobasal degeneration. *Brain Pathol.* **11**, 144–158 (2001).
72. Sawamura, N. *et al.* Site-specific phosphorylation of tau accompanied by activation of mitogen-activated protein kinase (MAPK) in brains of Niemann–Pick type C mice. *J. Biol. Chem.* **276**, 10314–10319 (2001).
73. Takashima, A., Noguchi, K., Sato, K., Hoshino, T. & Imahori, K. Tau protein kinase I is essential for amyloid β-protein-induced neurotoxicity. *Proc. Natl Acad. Sci. USA* **90**, 7789–7793 (1993).
74. Takashima, A. *et al.* Exposure of rat hippocampal neurons to amyloid β peptide (25–35) induces the inactivation of phosphatidyl inositol-3 kinase and the activation of tau protein kinase I/glycogen synthase kinase-3 β. *Neurosci. Lett.* **203**, 33–36 (1996).
75. Takashima, A. *et al.* Activation of tau protein kinase I/glycogen synthase kinase-3β by amyloid β peptide (25–35) enhances phosphorylation of tau in hippocampal neurons. *Neurosci. Res.* **31**, 317–323 (1998).
76. Ferreira, A., Lu, Q., Orecchio, L. & Kosik, K. S. Selective phosphorylation of adult tau isoforms in mature hippocampal neurons exposed to fibrillar A β. *Mol. Cell. Neurosci.* **9**, 220–234 (1997).
77. Lee, M. S. *et al.* APP processing is regulated by cytoplasmic phosphorylation. *J. Cell Biol.* **163**, 83–95 (2003).
78. Otth, C. *et al.* AβPP induces cdk5-dependent tau hyperphosphorylation in transgenic mice Tg2576. *J. Alzheimers Dis.* **4**, 417–430 (2002).
79. Alvarez, A., Toro, R., Caceres, A. & Maccioni, R. B. Inhibition of tau phosphorylating protein kinase cdk5 prevents β-amyloid-induced neuronal death. *FEBS Lett.* **459**, 421–426 (1999).
80. Town, T. *et al.* p35/Cdk5 pathway mediates soluble amyloid-β peptide-induced tau phosphorylation *in vitro*. *J. Neurosci. Res.* **69**, 362–372 (2002).
81. Ryder, J. *et al.* Divergent roles of GSK3 and CDK5 in APP processing. *Biochem. Biophys. Res. Commun.* **312**, 922–929 (2003).
82. Alvarez, G. *et al.* Lithium protects cultured neurons against β-amyloid-induced neurodegeneration. *FEBS Lett.* **453**, 260–264 (1999).
83. Hoshi, M. *et al.* Spherical aggregates of β-amyloid (amylospheroid) show high neurotoxicity and activate tau protein kinase I/glycogen synthase kinase-3β. *Proc. Natl Acad. Sci. USA* **100**, 6370–6375 (2003).
84. Fillit, H. M. & Refolo, L. M. Advancing drug discovery for Alzheimer's disease. *Curr. Alzheimer Res.* **2**, 105–107 (2005).
85. Hung, K.S. *et al.* Calpain inhibitor inhibits p35–p25–Cdk5 activation, decreases tau hyperphosphorylation, and improves neurological function after spinal cord hemisection in rats. *J. Neuropathol. Exp. Neurol.* **64**, 15–26 (2005).
86. Gould, T. D. & Manji, H. K. Glycogen synthase kinase-3: a putative molecular target for lithium mimetic drugs. *Neuropsychopharmacol.* **30**, 1223–1237 (2005).
87. Noble, W. *et al.* Inhibition of glycogen synthase kinase-3 by lithium correlates with reduced tauopathy and degeneration *in vivo*. *Proc. Natl Acad. Sci. USA* **102**, 6990–6995 (2005).
The *in vivo* effects of lithium on tau hyperphosphorylation support the idea that kinases are involved in tauopathy progression and that kinase inhibitors may be effective therapeutically.
88. Nakashima, H. *et al.* Chronic lithium treatment decreases tau lesions by promoting ubiquitination in a mouse model of tauopathies. *Acta Neuropathol.* **110**, 547–556 (2005).
89. Pickhardt, M. *et al.* Anthraquinones inhibit tau aggregation and dissolve Alzheimer's paired helical filaments *in vitro* and in cells. *J. Biol. Chem.* **280**, 3628–3635 (2005).
90. Khlistunova, I. *et al.* Inducible expression of Tau repeat domain in cell models of tauopathy: aggregation is toxic to cells but can be reversed by inhibitor drugs. *J. Biol. Chem.* **281**, 1205–1214 (2006).
Suggests that pharmacological agents may be able to prevent tau aggregation and may even dissolve preformed tau aggregates.
91. Lewis, J. *et al.* Neurofibrillary tangles, amyotrophy and progressive motor disturbance in mice expressing mutant (P301L) tau protein. *Nature Genet.* **25**, 402–405 (2000).
92. Patel, S., Doble, B. & Woodgett, J. R. Glycogen synthase kinase-3 in insulin and Wnt signalling: a double-edged sword? *Biochem. Soc. Trans.* **32**, 803–808 (2004).
93. Fischer, P. M. Cyclin-dependent kinase inhibitors: discovery, development and target rationale for different therapeutic applications. *Drugs Fut.* **30**, 911–929 (2005).
94. Weishaupt, J. H. *et al.* Inhibition of CDK5 is protective in necrotic and apoptotic paradigms of neuronal cell death and prevents mitochondrial dysfunction. *Mol. Cell. Neurosci.* **24**, 489–502 (2003).
95. Gillardon, F., Schrattenholz, A. & Sommer, B. Investigating the neuroprotective mechanism of action of a CDK5 inhibitor by phosphoproteome analysis. *J. Cell. Biochem.* **95**, 817–826 (2005).
96. Manning, G., Whyte, D. B., Martinez, R., Hunter, T. & Sudarsanam, S. The protein kinase complement of the human genome. *Science* **298**, 1912–1934 (2002).
97. McInnes, C. & Fischer, P. M. Strategies for the design of potent and selective kinase inhibitors. *Curr. Pharm. Des.* **11**, 1845–1863 (2005).
98. Fischer, P. M. The design of drug candidate molecules as selective inhibitors of therapeutically relevant kinases. *Curr. Med. Chem.* **11**, 1563–1583 (2004).
99. Hanks, S. K. & Hunter, T. Protein kinases 6. The eukaryotic protein kinase superfamily: kinase (catalytic) domain structure and classification. *FASEB J.* **9**, 576–596 (1995).
100. Jeffrey, P. D. *et al.* Mechanism of CDK activation revealed by the structure of a cyclinA-CDK2 complex. *Nature* **376**, 313–320 (1995).
101. Otyepka, M., Bartova, I., Kriz, Z. & Koca, J. Different mechanisms of CDK5 and CDK2 activation as revealed by CDK5/p25 and CDK2/cyclin A dynamics. *J. Biol. Chem.* **281**, 7271–7281 (2006).
102. Mapelli, M. *et al.* Mechanism of CDK5/p25 binding by CDK inhibitors. *J. Med. Chem.* **48**, 671–679 (2005).
Seminal paper on structure-based design of CDK5 inhibitors.
103. Tarricone, C. *et al.* Structure and regulation of the CDK5–p25(nck5a) complex. *Mol. Cell* **8**, 657–669 (2001).
104. Capdeville, R., Buchdunger, E., Zimmermann, J. & Matter, A. Glivec (STI571, imatinib), a rationally developed, targeted anticancer drug. *Nature Rev. Drug. Discov.* **1**, 493–502 (2002).

© 2007 **Nature Publishing Group**

105. Liu, Y. & Gray, N. S. Rational design of inhibitors that bind to inactive kinase conformations. *Nature Chem. Biol.* **2**, 358–364 (2006).
106. Heron, N. M. *et al.* SAR and inhibitor complex structure determination of a novel class of potent and specific Aurora kinase inhibitors. *Bioorg. Med. Chem. Lett.* **16**, 1320–1323 (2006).
107. Johnson, K. *et al.* Inhibition of neuronal apoptosis by the cyclin-dependent kinase inhibitor GW8510: Identification of 3′ substituted indolones as a scaffold for the development of neuroprotective drugs. *J. Neurochem.* **93**, 538–548 (2005).
108. Hoessel, R. *et al.* Indirubin, the active constituent of a Chinese antileukaemia medicine, inhibits cyclin-dependent kinases. *Nature Cell Biol.* **1**, 60–67 (1999).
109. Meijer, L. & Raymond, E. Roscovitine and other purines as kinase inhibitors. From starfish oocytes to clinical trials. *Acc. Chem. Res.* **36**, 417–425 (2003).
110. Mettey, Y. *et al.* Aloisines, a new family of CDK/GSK-3 inhibitors. SAR study, crystal structure in complex with CDK2, enzyme selectivity and cellular effects. *J. Med. Chem.* **46**, 222–236 (2003).
111. Kinoshita, T. *et al.* Crystal structure of human ERK2 complexed with a pyrazolo[3,4-*c*]pyridazine derivative. *Bioorg. Med. Chem. Lett.* **16**, 55–58 (2006).
First paper to shed light on the design of ERK2-specific kinase inhibitors.
112. Xiao, Z., Hao, Y., Liu, B. & Qian, L. Indirubin and meisoindigo in the treatment of chronic myelogenous leukemia in China. *Leuk. Lymph.* **43**, 1763–1768 (2002).
113. Fischer, P. M. CDK versus GSK-3 inhibition: a purple haze no longer? *Chem. Biol.* **10**, 1144–1146 (2003).
114. Leclerc, S. *et al.* Indirubins inhibit glycogen synthase kinase-3β and CDK5/P25, two protein kinases involved in abnormal tau phosphorylation in Alzheimer's disease A property common to most cyclin-dependent kinase inhibitors? *J. Biol. Chem.* **276**, 251–260 (2001).
SARs of indirubins with respect to GSK3β and CDK5 inhibition; this paper confirms inhibition of tau phosphorylation at sites relevant to tau hyperphosphorylation in AD.
115. Polychronopoulos, P. *et al.* Structural basis for the synthesis of indirubins as potent and selective inhibitors of glycogen synthase kinase-3 and cyclin-dependent kinases. *J. Med. Chem.* **47**, 935–946 (2004).
116. Meijer, L. *et al.* GSK-3-selective inhibitors derived from tyrian purple indirubins. *Chem. Biol.* **10**, 1255–1266 (2003).
117. Marko, D. *et al.* Inhibition of cyclin-dependent kinase 1 (CDK1) by indirubin derivatives in human tumour cells. *Br. J. Cancer* **84**, 283–289 (2001).
118. Davies, T. G. *et al.* Inhibitor binding to active and inactive CDK2: the crystal structure of CDK2-cyclin A/indirubin-5-sulphonate. *Structure* **9**, 389–397 (2001).
119. Damiens, E., Baratte, B., Marie, D., Eisenbrand, G. & Meijer, L. Anti-mitotic properties of indirubin-3′-monoxime, a CDK/GSK-3 inhibitor: induction of endoreplication following prophase arrest. *Oncogene* **20**, 3786–3797 (2001).
120. Heredia, A. *et al.* Indirubin-3′-monoxime, a derivative of a Chinese antileukemia medicine, inhibits P-TEFb function and HIV-1 replication. *AIDS* **19**, 2087–2095 (2005).
121. Huang, M., Wang, Y., Cogut, S. B., Mitchell, B. S. & Graves, L. M. Inhibition of nucleoside transport by protein kinase inhibitors. *J. Pharmacol. Exp. Ther.* **304**, 753–760 (2003).
122. Adachi, J. *et al.* Indirubin and indigo are potent aryl hydrocarbon receptor ligands present in human urine. *J. Biol. Chem.* **276**, 31475–31478 (2001).
123. Knockaert, M. *et al.* Independent actions on cyclin-dependent kinases and aryl hydrocarbon receptor mediate the antiproliferative effects of indirubins. *Oncogene* **23**, 4400–4412 (2004).
124. Jautelat, R. *et al.* From the insoluble dye indirubin towards highly active, soluble CDK2-inhibitors. *ChemBioChem* **6**, 531–540 (2005).
125. De Azevedo, W. F. *et al.* Inhibition of cyclin-dependent kinases by purine analogues: crystal structure of human cdk2 complexed with roscovitine. *Eur. J. Biochem.* **243**, 518–526 (1997).
126. De Azevedo, W. F. Jr, Canduri, F. & Da Silveira, N. J. F. Structural basis for inhibition of cyclin-dependent kinase 9 by flavopiridol. *Biochem. Biophys. Res. Commun.* **293**, 566–571 (2002).
127. Legraverend, M. *et al.* Cyclin-dependent kinase inhibition by new C-2 alynylated purine derivatives and molecular structure of a CDK2-inhibitor complex. *J. Med. Chem.* **43**, 1282–1292 (2000).
128. Dreyer, M. K. *et al.* Crystal structure of human cyclin-dependent kinase 2 in complex with the adenine-derived inhibitor H717. *J. Med. Chem.* **44**, 524–530 (2001).
129. Arris, C. E. *et al.* Identification of novel purine and pyrimidine cyclin-dependent kinase inhibitors with distinct molecular interactions and tumor cell growth inhibition profiles. *J. Med. Chem.* **43**, 2797–2804 (2000).
130. Vesely, J. *et al.* Inhibition of cyclin-dependent kinases by purine analogues. *Eur. J. Biochem.* **224**, 771–786 (1994).
131. Wang, Z. *et al.* Structural basis of inhibitor selectivity in MAP kinases. *Structure* **6**, 1117–1128 (1998).
132. Gray, N. S. *et al.* Exploiting chemical libraries, structure, and genomics in the search for kinase inhibitors. *Science* **281**, 533–538 (1998).
133. Chang, Y. T. *et al.* Synthesis and application of functionally diverse 2,6,9-trisubstituted purine libraries as CDK inhibitors. *Chem. Biol.* **6**, 361–375 (1999).
134. Schulze-Gahmen, U. *et al.* Multiple modes of ligand recognition: crystal structures of cyclin-dependent protein kinase 2 in complex with ATP and two inhibitors, olomucine and isopentyladenine. *Proteins* **22**, 378–391 (1995).
135. Shum, P. W. *et al.* The design and synthesis of purine inhibitors of CDK2. III. *Nucleosides, Nucleotides Nucleic Acids* **20**, 1067–1078 (2001).
136. Ohori, M. *et al.* Identification of a selective ERK inhibitor and structural determination of the inhibitor-ERK2 complex. *Biochem. Biophys. Res. Commun.* **336**, 357–363 (2005).
137. Martinez, A., Alonso, M., Castro, A., Perez, C. & Moreno, F. J. First non-ATP competitive glycogen synthase kinase 3β (GSK-3β) inhibitors: thiadiazolidinones (TDZD) as potential drugs for the treatment of Alzheimer's disease. *J. Med. Chem.* **45**, 1292–1299 (2002).
138. Martinez, A. *et al.* SAR and 3D-QSAR studies on thiadiazolidinone derivatives: exploration of structural requirements for glycogen synthase kinase 3 inhibitors. *J. Med. Chem.* **48**, 7103–7112 (2005).
139. Cohen, M. S., Zhang, C., Shokat, K. M. & Taunton, J. Structural bioinformatics-based design of selective, irreversible kinase inhibitors. *Science* **308**, 1318–1321 (2005).
140. Conde, S., Perez, D. I., Martinez, A., Perez, C. & Moreno, F. J. Thienyl and phenyl α-halomethyl ketones: new inhibitors of glycogen synthase kinase (GSK-3β) from a library of compound searching. *J. Med. Chem.* **46**, 4631–4633 (2003).
141. Ahn, J. S. *et al.* Defining Cdk5 ligand chemical space with small molecule inhibitors of tau phosphorylation. *Chem. Biol.* **12**, 811–823 (2005).
142. Sharma, P. *et al.* Identification of substrate binding site of cyclin-dependent kinase 5. *J. Biol. Chem.* **274**, 9600–9606 (1999).
143. Chin, K. T. *et al.* Identification and structure characterization of a Cdk inhibitory peptide derived from neuronal-specific Cdk5 activator. *J. Biol. Chem.* **274**, 7120–7127 (1999).
144. Kesavapany, S. *et al.* Neuronal cyclin-dependent kinase 5: role in nervous system function and its specific inhibition by the Cdk5 inhibitory peptide. *Biochim. Biophys. Acta* **1697**, 143–153 (2004).
145. Amin, N. D., Albers, W. & Pant, H. C. Cyclin-dependent kinase 5 (cdk5) activation requires interaction with three domains of p35. *J. Neurosci. Res.* **67**, 354–362 (2002).
146. Zheng, Y. L., Li, B. S., Amin, N. D., Albers, W. & Pant, H. C. A peptide derived from cyclin-dependent kinase activator (p35) specifically inhibits Cdk5 activity and phosphorylation of tau protein in transfected cells. *Eur. J. Biochem.* **269**, 4427–4434 (2002).
147. Zheng, Y.-L. *et al.* A Cdk5 inhibitory peptide reduces tau hyperphosphorylation and apoptosis in neurons. *EMBO J.* **24**, 209–220 (2005).
Outlines a potential alternative therapeutic strategy for CDK5 inhibition that does not involve ATP-competitive inhibitors.
148. Molina, D. M., Grewal, S. & Bardwell, L. Characterization of an ERK-binding domain in microphthalmia-associated transcription factor and differential inhibition of ERK2-mediated substrate phosphorylation. *J. Biol. Chem.* **280**, 42051–42060 (2005).
149. Lipinski, C. A. Filtering in drug discovery. *Ann. Rep. Comput. Chem.* **1**, 155–168 (2005).
150. Bertrand, J. A. *et al.* Structural characterization of the GSK-3β active site using selective and non-selective ATP-mimetic inhibitors. *J. Mol. Biol.* **333**, 393–407 (2003).
151. Brown, N. R. *et al.* Effects of phosphorylation of threonine 160 on cyclin-dependent kinase 2 structure and activity. *J. Biol. Chem.* **274**, 8746–8756 (1999).
152. ter Haar, E. *et al.* Structure of GSK3β reveals a primed phosphorylation mechanism. *Nature Struct. Biol.* **8**, 593–596 (2001).
153. Davies, T. G. *et al.* Structure-based design of a potent purine-based cyclin-dependent kinase inhibitor. *Nature Struct. Biol.* **9**, 745–749 (2002).
154. Clare, P. M. *et al.* The cyclin-dependent kinases cdk2 and cdk5 act by a random, anticooperative kinetic mechanism. *J. Biol. Chem.* **276**, 48292–48299 (2001).
155. Bramson, H. N. *et al.* Oxindole-based inhibitors of cyclin-dependent kinase 2 (CDK2): design, synthesis, enzymatic activities and X-ray crystallographic analysis. *J. Med. Chem.* **44**, 4339–4358 (2001).
156. Richardson, C. M. *et al.* Triazolo[1,5-*a*]pyrimidines as novel CDK2 inhibitors: protein structure-guided design and SAR. *Bioorg. Med. Chem. Lett.* **16**, 1353–1357 (2006).
157. Brown, N. R., Noble, M. E., Endicott, J. A. & Johnson, L. N. The structural basis for specificity of substrate and recruitment peptides for cyclin-dependent kinases. *Nature Cell Biol.* **1**, 438–443 (1999).
158. Helal, C. J. *et al.* Discovery and SAR of 2-aminothiazole inhibitors of cyclin-dependent kinase 5/p25 as a potential treatment for Alzheimer's disease. *Bioorg. Med. Chem. Lett.* **14**, 5521–5525 (2004).
159. Leost, M. *et al.* Paullones are potent inhibitors of glycogen synthase kinase-3β and cyclin-dependent kinase 5/p25. *Eur. J. Biochem.* **267**, 5983–5994 (2000).
Describes ATP-competitive inhibition of CDK5–p25 and GSK3 by paullones and the resulting effects on tau phosphorylation *in vitro* and *in vivo*.
160. Sondhi, S. M. *et al.* Synthesis of acridinyl-thiazolino derivatives and their evaluation for anti-inflammatory, analgesic and kinase inhibition activities. *Bioorg. Med. Chem.* **13**, 4291–4299 (2005).
161. Voigt, B. *et al.* Novel CDK inhibition profiles of structurally varied 1-aza-9-oxafluorenes. *Bioorg. Med. Chem. Lett.* **15**, 823–825 (2005).
162. Engler, T. A. *et al.* Novel, potent and selective cyclin D1/CDK4 inhibitors: indolo[6,7-*a*]pyrrolo[3,4-*c*]carbazoles. *Bioorg. Med. Chem. Lett.* **13**, 2261–2267 (2003).
163. Clark, D. E. Computational prediction of blood–brain barrier permeation. *Annu. Rep. Med. Chem.* **40**, 403–415 (2005).
164. Norinder, U. & Haeberlein, M. Computational approaches to the prediction of the blood–brain distribution. *Adv. Drug Delivery Rev.* **54**, 291–313 (2002).

Competing interests statement
The authors declare no competing financial interests.

DATABASES
The following terms in this article are linked online to:
Entrez Gene: http://www.ncbi.nlm.nih.gov/entrez/query.fcgi?db=gene
CDK5 | ERK2 | GSK3β | tau

FURTHER INFORMATION
PyMol program: http://www.pymol.org
Access to this links box is available online.

© 2007 Nature Publishing Group